

**Summary Report**

**Low Temperature and Thermal Fatigue Cracking  
SR-OSU-A-003A-89-1**

**by**

**Ted S. Vinson  
Professor of Civil Engineering  
Oregon State University  
Corvallis, OR 97331**

**Vincent C. Janoo  
Research Engineer  
US Army Cold Regions Research and Engineering Lab  
Hanover, NH 03755**

**and**

**Ralph C.G. Haas  
Professor of Civil Engineering  
University of Waterloo  
Waterloo, Ontario N2L 3G1**

**June 1989**

## ABSTRACT

Cracking of asphalt concrete pavements owing to cold temperatures or temperature cycling can occur in many regions of the United States. Cracking that results from cold temperatures generally is referred to as low temperature cracking; cracking that results from thermal cycling generally is referred to as thermal fatigue cracking. Thermal cracks permit the ingress of water, which may result in a depression at the crack because of the pumping of support materials. During the winter months, deicing solutions can enter the cracks and cause localized thawing of the base and a depression at the crack. Water entering the crack also may freeze, resulting in the formation of an ice lens, which can produce upward lipping at the crack edge. All of these effects result in poor ride quality and reduction in pavement life.

Under a long term research program to develop test methods which are suitable to accurately and reliably characterize the engineering properties of asphalt-aggregate mixtures, an exhaustive literature review and an analysis of responses to a survey questionnaire was conducted to identify test methods that are currently used to predict low temperature and thermal fatigue cracking in asphalt concrete pavements. Eight test systems/methods were identified. These methods were evaluated in terms of the following criteria:

- Simulation of field conditions
- Application of test results to mechanistic models
- Suitability for aging and moisture conditioning
- Potential to accommodate large stone mixes
- Ease of conduct
- Cost of equipment

Based on the evaluation of the test systems/methods presented, it would appear that four test systems/methods warrant further consideration in a laboratory test program, as follows:

- Direct Tension–Constant Rate of Extension test
- Thermal Stress Restrained Specimen test
- C\*–Line Integral test
- Coefficient of Thermal Expansion and Contraction test

A test program is identified which should be conducted to provide a preliminary evaluation of the availability of selected test systems/methods (1) for standardization, and (2) to provide input parameters to mechanistic models for low temperature and thermal fatigue cracking.

## ACKNOWLEDGEMENTS

The work reported herein has been conducted as a part of project A-003A of the Strategic Highway Research Program (SHRP). SHRP is a unit of the National Research Council that was authorized by section 128 of the Surface Transportation and Uniform Relocation Assistance Act of 1987. This project is entitled, "Performance Related Testing and Measuring of Asphalt-Aggregate Interactions and Mixtures," and is being conducted by the Institute of Transportation Studies, University of California, Berkeley, with Carl L. Monismith as Principal Investigator. The support and encouragement of Ian Jamieson, SHRP Contract Manager, is gratefully acknowledged. Peter Bellin, SHRP Staff Engineer, was particularly helpful in identifying related work performed by the West German pavement-engineering research community.

The draft of this report was reviewed by an Expert Task Group (ETG), which provided many valuable comments. The members are:

Ernest Bastian  
Federal Highway Administration

Campbell Crawford  
National Asphalt Paving Association

William Dearasaugh  
Transportation Research Board

Francis Fee  
ELF Asphalt

Douglas I. Hanson  
New Mexico State Highway Dept.

Eric E. Harm  
Illinois Dept. of Transportation

Charles S. Hughes  
Virginia Highway & Transportation  
Research Council

Dallas N. Little  
Texas A&M University

Kevin Stuart  
Federal Highway Administration

Roger L. Yarbrough  
University Asphalt Company

## **DISCLAIMER**

The contents of this report reflect the views of the authors, who are solely responsible for the facts and accuracy of the data presented. The contents do not necessarily reflect the official view or policies of the Strategic Highway Research Program (SHRP) or SHRP's sponsors. The results reported here are not necessarily in agreement with the results of other SHRP research activities. They are reported to stimulate review and discussion within the research community. This report does not constitute a standard, specification, or regulation.

## TABLE OF CONTENTS

	<u>Page</u>
1.0 INTRODUCTION . . . . .	1
1.1 Problem Definition . . . . .	1
1.2 Purpose of Report . . . . .	3
2.0 BACKGROUND . . . . .	4
2.1 Methodology . . . . .	4
2.2 Low Temperature Cracking . . . . .	4
2.3 Thermal Fatigue Cracking . . . . .	19
2.4 Summary of Factors Influencing Response . . . . .	25
2.5 Regression Equations to Predict Thermal Cracking . . . . .	29
3.0 DESCRIPTION OF TEST SYSTEMS ANDN METHODS . . . . .	34
3.1 Indirect Diametral Tesion Test . . . . .	34
3.2 Direct Tension – Constant Rate of Extension . . . . .	36
3.3 Tensile Creep Test . . . . .	38
3.4 Flexural Bending Test . . . . .	39
3.5 Thermal Stress Retained Specimen Test . . . . .	42
3.6 Three–Point Bend Specimen Test . . . . .	49
3.7 C*–Line Integral Test . . . . .	55
3.8 Coefficient of Thermal Expansion and Contraction Test . . . . .	59
3.9 Determination of Thermal Conductivity and Specific Heat Capacity . . . . .	62
4.0 RELATIONSHIP BETWEEN TEST PROCEDURES and FIELD PERFORMANCE . . . . .	63
4.1 Description of Mechanistic Models . . . . .	63
4.2 Input and Output Data for Mechanistic Models . . . . .	67

5.0 EVALUATION OF TEST METHODS AND PROPOSED TEST PROGRAM . . . . . 70

    5.1 Evaluation of Test Methods . . . . . 70

    5.2 Proposed Test Program . . . . . 73

6.0 CONCLUSIONS AND RECOMMENDATIONS . . . . . 78

    6.1 Preliminary Conclusions . . . . . 78

    6.2 Recommendations . . . . . 78

REFERENCES . . . . . 79

## LIST OF FIGURES

<u>Figure</u>		<u>Page</u>
1	Cross Section of Cold Pavement Showing Temperature and Thermal Stress Gradients (after Haas, et. al., 1987) . . . . .	2
2	Plan View of Runway with Schematic Illustration of Typical Thermal Cracking Pattern (after Haas, et. al., 1987) . . . . .	2
3	Prediction of Fracture Temperature for a Restrained Strip of Asphalt Concrete . . . . .	5
4	Estimating the Fracture Temperature of an Asphaltic Concrete (after Hills and Brien, 1966) . . . . .	9
5	Stress-Temperature Relationships for Asphaltic Concretes (AC-1) (after Fabb, 1974) . . . . .	11
6	Thermal Fracture Tests on 10 Specimens (after Sugawara and Moriyoshi, 1984) . . . . .	12
7	Change of Temperature Induced Stress at Constant Low Temperature (after Sugawara and Moriyoshi, 1984) . . . . .	13
8	Change of Temperature Induced Stress at Second Cooling After 2 Hours Temperature Maintenance at Low Temperature (after Sugawara and Moriyoshi, 1984) . . . . .	14
9	Change of Temperature Induced Stress Under Cyclic Temperature Change (after Sugawara and Moriyoshi, 1984) . . . . .	16
10	Fracture Temperature as a Function of Aggregate Gradation, Asphalt Cement Content and Asphalt Viscosity (after Arand, 1989) . . . . .	17
11	Typical Expansion of Asphalt with Temperature Change (after Schmidt and Santucci, 1966) . . . . .	20
12	Temperature Ranges Associated with Different Types of Thermal Cracking (after Carpenter, 1983) . . . . .	21
13	Change of Thermal Stress and Fracture Under 120 Repetition of Cooling (between -20.5 and -25.5°C) (after Sugawara and Moriyoshi, 1984) . . . . .	22
14	Types of Transverse Cracking (after Fromm and Phang, 1972) .	31
15	Schematic of Diametral Tension Test Equipment (after Anderson and Leung, 1987) . . . . .	35



16	Schematic of Direct Tension and Creep Load Test Systems (after Haas, 1973)	
	(a) Overall Test System . . . . .	37
	(b) Constant Rate of Extension and Creep Load Frame . . . . .	37
17	Apparatus for Measuring Creep Deformation Under Constant Tensile Stress (after Fromm and Phang, 1972) . . . . .	39
18	Schematic of Thermal Stress Restrained Specimen Test (after Monismith, et. al., 1965)	
	(a) Thermal Stress Apparatus . . . . .	43
	(b) Controlled Temperature Cabinet for Thermal Stress Experiments . . . . .	43
19	Schematic of Thermal Stress Restrained Specimen Test (after Fabb, 1974) . . . . .	45
20	Schematic of Thermal Stress Restrained Specimen Test System (after Carpenter, 1983) . . . . .	47
21	USA CRREL Thermal Stress Restrained Specimen Test (after Janoo, 1989) . . . . .	48
22	Three-Point Bend Specimen (after Mahboub, 1985) . . . . .	51
23	Three-Point Bend Specimen Load versus Displacement (a) and Its Transformation to Moment versus Rotation (b) (after Mahboub, 1985) . . . . .	53
24	Illustration of Determination of Critical Energy Release Rate $J_{IC}$ , and Tearing Modulus, $T$ (after Mahboub, 1985) . . . . .	54
25	Steps in Determination of $C^*$ Line Integral (after Abdulshafi 1983b) . . . . .	56
26	Typical $C^*$ Test Configuration (after Abdulshafi, 1983b) . . . . .	58
27	Utah DOT Coefficient of Thermal Contraction Test Frame . . . . .	60
28	Flow Diagram for Program COLD (after Finn, et. al., 1986) . . . . .	64

## LIST OF TABLES

<u>Table</u>		<u>Page</u>
1	Summary of Input and Output Data for Low-Temperature Cracking Models (modified after Anderson, et al., 1989) . . .	68
2	Evaluation of Thermal Cracking Test Methodologies . . . . .	71
3	Proposed Test Programs for the Preliminary Evaluation of Test Systems/Methods . . . . .	75
4	Test and Material Variables for Load-Deformation Tests . . .	75
5	Test and Material Variables for Thermal Stress Restrained Specimen Tests . . . . .	76
6	Test and Material Variables for Thermal Cycle Restrained Specimen Tests . . . . .	76
7	Test and Material Variables for C*-Line Integral Tests . . .	77
8	Test and Material Variables for Coefficient of Thermal Expansion/Contraction Test . . . . .	77

## 1.0 INTRODUCTION

### 1.1 Problem Definition

Cracking of asphalt concrete pavements owing to cold temperatures or temperature cycling can occur in many regions of the United States. Cracking that results from cold temperatures generally is referred to as low temperature cracking; cracking that results from thermal cycling generally is referred to as thermal fatigue cracking. Low temperature cracking in North America typically is associated with the northern tier states, Canada, and Alaska. Thermal fatigue cracking generally is associated with areas that experience large extremes in daily temperatures, such as the southwestern and north central states.

The mechanism associated with low temperature cracking is simply that tensile stresses develop in an asphalt concrete pavement as the temperature drops to an extremely low value. When the tensile stress is equal to the tensile strength of the mixture at a given temperature, a micro crack develops at the surface of the pavement. The crack then propagates through the depth of the layer when subjected to additional thermal cycles. This situation is illustrated in Figure 1.

Low temperature cracking is transverse to the direction of traffic. Crack spacing can range from 3 to 300 ft. If the transverse crack spacing is less than the width of the pavement, longitudinal thermal cracking may occur, and a block pattern can develop, as shown in Figure 2. Also, longitudinal thermal cracks may develop along a paving lane joint since it represents a weak lineal feature in the pavement structure.

Thermal fatigue cracking may be associated with thermal cycling at moderate temperatures. Under daily temperature cycles, the temperature stress

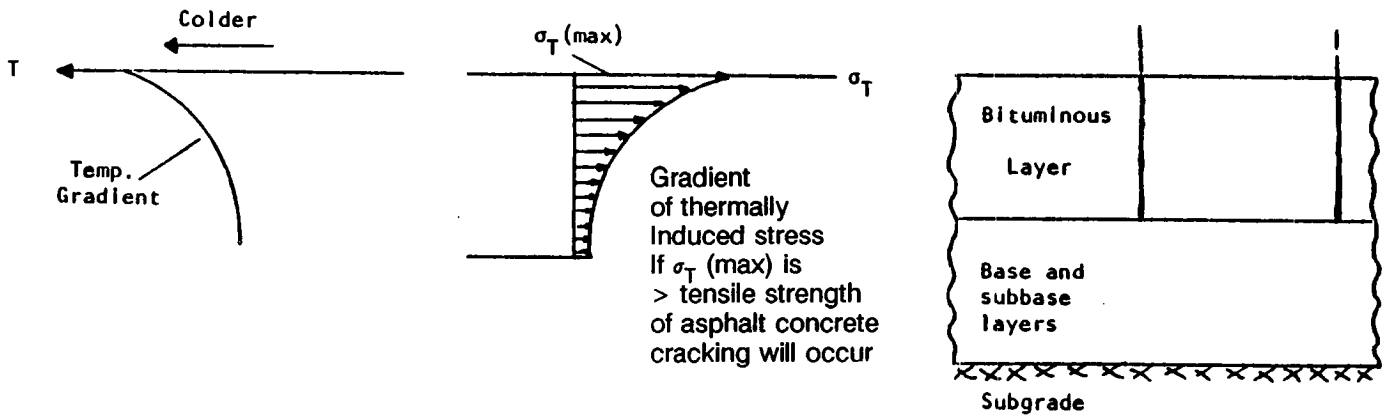


Figure 1. Cross Section of Cold Pavement Showing Temperature and Thermal Stress Gradients (after Haas, et al., 1987).

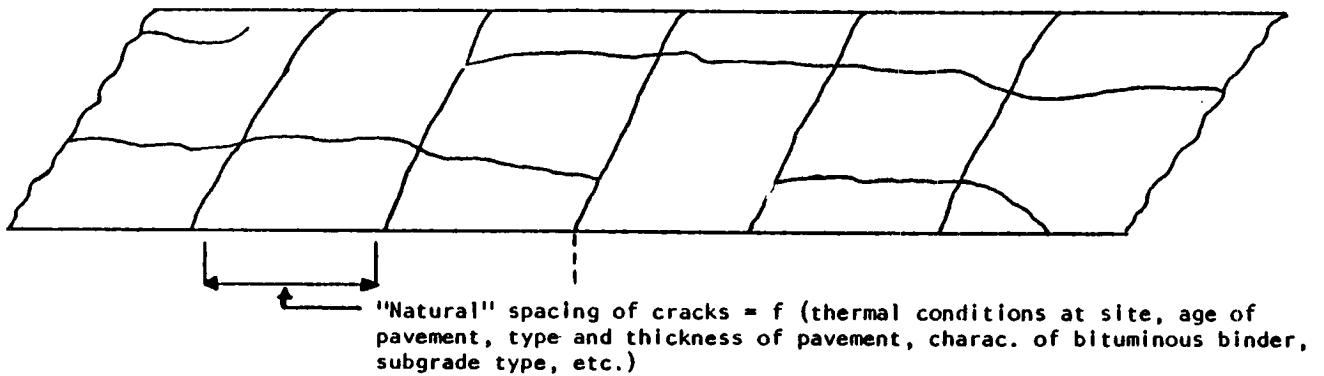


Figure 2. Plan View of Runway with Schematic Illustration of Typical Thermal Cracking Pattern (after Haas, et al., 1987).

is greatest at night and drops off during the warmer daytime temperature. Because the daily temperature cycling occurs at temperatures higher than those required for low temperature cracking, the stress in the pavement typically is far below the strength of the mixture at that temperature. Consequently, failure does not occur immediately, but develops over a period of time similar to the time required for fatigue cracking associated with traffic-load-induced strains in the asphalt concrete.

Thermal cracks permit the ingress of water, which may result in a depression at the crack because of the pumping of support materials. During the winter months, deicing solutions can enter the cracks and cause localized thawing of the base and a depression at the crack. Water entering the crack also may freeze, resulting in the formation of an ice lens, which can produce upward lipping at the crack edge. All of these effects result in poor ride quality and reduction in pavement life.

## **1.2 Purpose of Report**

The purpose of this report is to identify test methods that currently are used to predict low temperature and thermal fatigue cracking in asphalt concrete mixtures. Further, the test methods identified are documented and critically evaluated with respect to supporting a mechanistic approach to low temperature and thermal fatigue cracking. Finally, a test program that supports the evaluation of several of the test methods identified is defined. The report reflects the results of an exhaustive literature review and an analysis of the responses to a U.S. Army Cold Regions Research and Engineering Laboratory (USA CRREL) survey questionnaire sent to state Departments of Transportation relative to thermal cracking of pavements.

## **2.0 BACKGROUND**

### **2.1 Methodology**

Several computer searches (TRIS, MELVYL, COMPENDEX, COLD, DIALOG) were conducted to assist in locating all pertinent literature. A number of the documents noted in this report were identified in the search. The majority of the documents, however, were identified through the efforts of the principal investigator and the co-investigators on this subtask.

### **2.2 Low Temperature Cracking**

Low temperature cracking is associated with the volumetric contraction that occurs as a material experiences a temperature drop. If a material is unrestrained, it will shorten as the temperature drops. If a material is restrained, which is the case for asphalt concrete in a pavement structure, the tendency to shorten results in the development of a thermal stress that can produce cracking when the stress equals the tensile strength of the material. Asphalt concrete can be considered to act as a viscoelastic material at warm temperatures; consequently, the thermal stresses that develop when the temperature drops in a warm temperature range are dissipated through stress relaxation. However, in a low temperature range, the asphalt concrete behaves as an elastic material and the thermal stresses cannot dissipate and cracking can occur. This situation may be visualized as shown in Figure 3. The temperature at which failure occurs is referred to as the fracture temperature. Once failure has occurred and a crack develops, the stresses are relieved. In a new pavement, cracks generally have been observed to appear at 100+ ft spacing. As the pavement ages and/or more extreme temperature drops occur, the crack spacing has been observed to decrease to 10-20 ft.

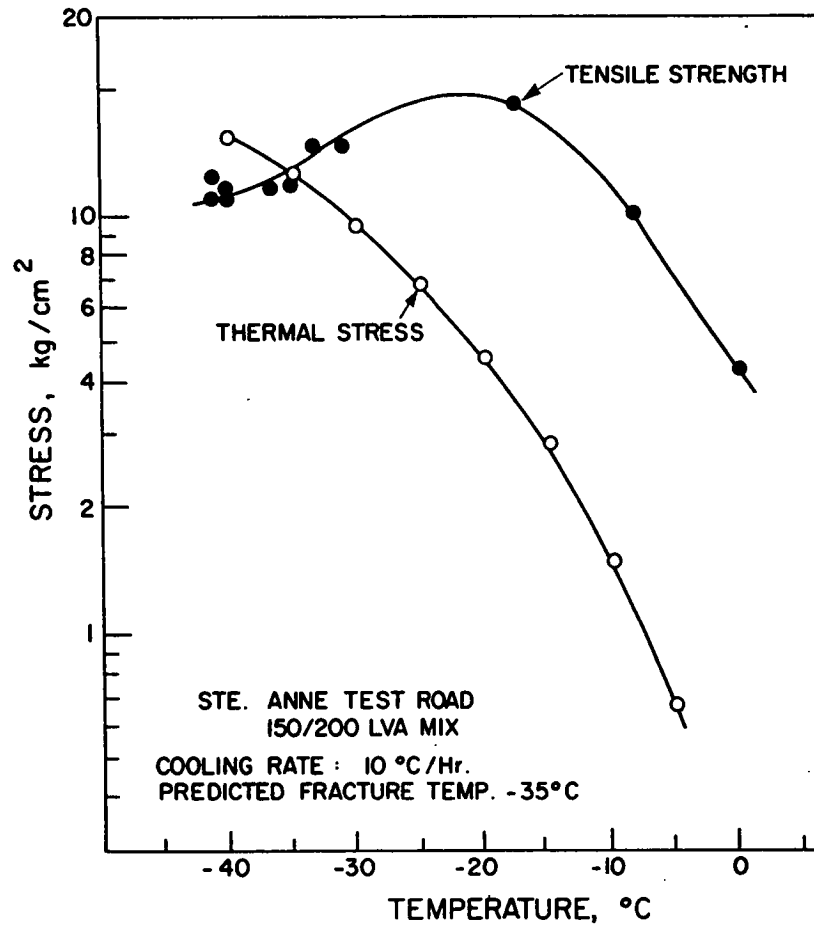


Figure 3. Prediction of Fracture Temperature for a Restrained Strip of Asphalt Concrete.

The calculation of the thermal stress has been approximated by Hills and Brien (1966) using the following equation:

$$\sigma(\dot{T}) = \alpha \sum_{T_0}^{T_f} S(t,T) \cdot \Delta T \quad (1)$$

in which,

- $\sigma(\dot{T})$  = accumulated, thermally induced stress for a particular cooling rate,  $\dot{T}$ ,
- $\alpha$  = coefficient of thermal contraction (averaged over the temperature drop,  $T_0 - T_f$ , typical range 2 to  $2.5 \times 10^{-5}/^{\circ}\text{C}$ ),
- $T_0$  = initial temperature,
- $T_f$  = final temperature,
- $S(t,T)$  = asphalt mix stiffness (modulus), which is both time- and temperature-dependent, thereby recognizing the visco-elastic nature of the material,
- $\Delta T$  = temperature increment over which  $S(t,T)$  is applicable.

The stress calculated from Eq. (1) is associated with an infinite, completely restrained strip. More rigorous solutions to the problem are available. For example, Monismith, et al., (1965) used the stress equation developed by Humphreys and Martin (1963) to predict the stresses in a slab composed of a linear viscoelastic material subjected to a time-dependent temperature field. The slab was assumed to be of infinite lateral extent and completely restrained. However, the stresses that are predicted may be unrealistically high (Haas and Topper, 1969). If the solution is modified to use the assumption of a long beam instead of a slab, the computed stresses are slightly underestimated (Haas, 1973).



The approximate solution suggested by equation (1), which has been called the pseudo-elastic beam analysis, yields reasonable results (Christison and Anderson, 1972; Christison, et al., 1972). Further, the approximate solution has been extended by Haas and Topper (1969) to include both temperature and stiffness gradients through the depth of the bituminous layer. It also has been used to calculate thermally induced stresses and to predict the fracture temperature at the Ste. Anne Test Road (Burgess, et al., 1971) and the Arkona Test Road (Haas, 1970; Haas and Phang, 1988). Finally, the approximate solution supports the methodology of the COLD model to predict low temperature cracking (Finn, et al., 1986).

The thermal stress relationship shown in Figure 3 may be obtained by indirect estimation. For example, the binder stiffness-temperature relationship at an appropriate (but arbitrary) loading time, may be estimated from the Penetration Index and softening point values and van der Poel's (1954) nomogram. Then the asphalt mix stiffness-temperature relationship is calculated from Heukelom and Klomp's (1964) data, which give asphalt mix stiffness as a function of the binder stiffness and the volume concentration ( $C_v$ ) of the aggregate in the asphalt mix. With a measured or assumed coefficient of thermal expansion for the asphalt and the asphalt mix stiffness-temperature relationship, a stress-temperature relationship is obtained from equation (1). Variations on this approach are given in the literature (Haas, 1973) based on Heukelom's (1969) or McLeod's (1972) bitumen consistency versus temperature relationship.

Another form of indirect estimation of the thermal stress relationship is associated with the use of the load-deformation response (and associated stress-strain response) of asphalt concrete specimens obtained over a range of cold temperatures. Creep (Monismith, et al., 1965; Fromm and Phang, 1972;

Haas, 1973; and others), flexural bending (Busby and Rader, 1972), direct tension (Haas, 1973; Kallas, 1982), and indirect diametral tension (Christison, et al., 1972; Anderson and Leung, 1987; and others) tests all have been used to measure the stress-strain response of an asphalt concrete mix. Multiplying the stress-strain response of the mix (at a specified rate of loading and time) by the measured or assumed coefficient of thermal expansion gives the thermal stress relationship as shown in Figure 4. The fundamental limitation with the use of the load-deformation test methods noted is the identification of a rate of loading that corresponds to a rate of temperature drop in the field. Haas (1973) suggests that the modulus should be evaluated at a specific temperature, which represents the midpoint of a discrete temperature interval,  $\Delta T$ , using a loading time that corresponds to the time interval for the temperature interval.

Alternatively, the development of thermal stresses may be measured directly in the laboratory (Monismith, et al., 1965; Fabb, 1974; Sugawara and Moriyoshi, 1984; Arand, 1987; and others). This is accomplished by measuring the stress (force divided by specimen area) required to maintain a specimen at constant length under a specified rate of cooling. A comparison of measured to calculated thermal stresses by Hills and Brien (1966) is given in Figure 4. The direct measurement procedure eliminates the need to measure or assume a coefficient of thermal expansion for the mix.

The tensile strength of the asphalt mix may be estimated directly from relationships recorded by Heukelom and Klomp (1966). The tensile strength relationship also has been determined in the laboratory with both the direct tension test (Haas, 1973; Kallas, 1982) and indirect diametral test methods (Christison, et al., 1972; Anderson and Leung, 1987; and others).

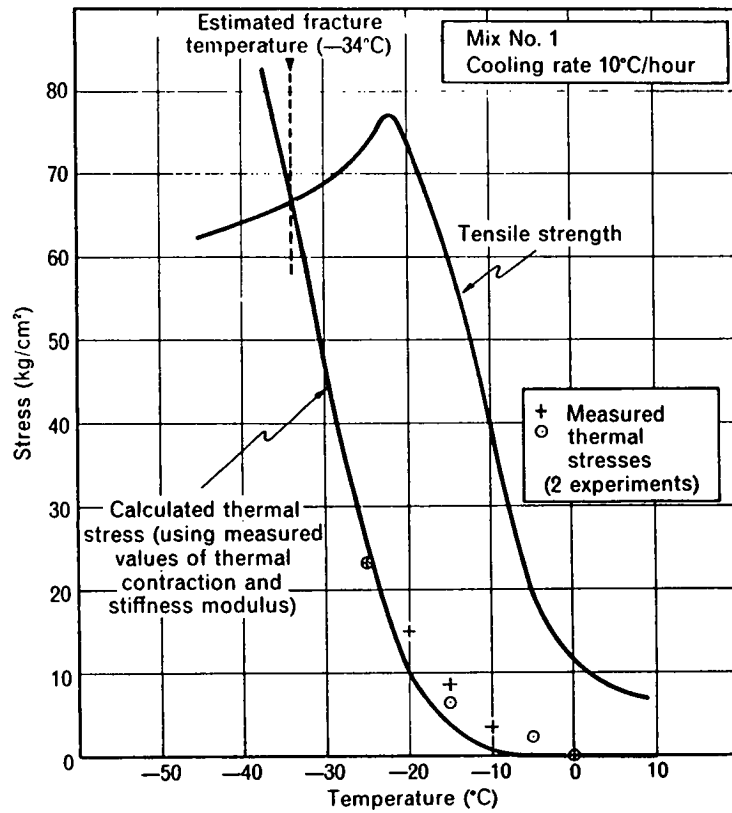


Figure 4. Estimating the Fracture Temperature of an Asphaltic Concrete (after Hills and Brien, 1966).

With knowledge of the thermal stress and tensile strength relationships, the fracture temperature may be estimated as the temperature at which the thermal stress equals the tensile strength as the temperature drops.

It also is possible to measure thermally-induced fracture stresses and fracture temperature in the laboratory (Fabb, 1974; Sugawara and Moriyoshi, 1984). Typical test results are shown in Figure 5. Fabb recorded failure temperatures between  $-25$  and  $-40^{\circ}\text{C}$  and stated that failure temperatures are closely related to the "hardness" and rheological characteristics of the asphalt cement. Fabb considered three cooling rates (5, 10, and  $27^{\circ}\text{C/hr}$ ) and concluded that the rate of cooling has little or no effect on the failure temperature. (These rates of cooling are significantly greater than experienced in the field, and a lower rate of cooling may affect failure stresses and temperature.) Bloy (1980) established that differences in rates of cooling below  $5^{\circ}\text{C/hr}$  influenced the temperature at which cracking occurred in asphalt cements, whereas differences in rates of cooling above  $5^{\circ}\text{C/hr}$  had no influence. The repeatability of thermal fracture tests is suggested by the results presented in Figure 6. Sugawara and Moriyoshi (1984) attribute the minor differences in the fracture temperature and strength to differences in the fracture mechanism at low temperatures.

The influence of thermal history on induced stress was investigated by Sugawara and Moriyoshi (1984). The results from their research are shown in Figures 7, 8, and 9. The results shown in Figure 7 reflect cooling down to a given temperature then maintaining the temperature for 20 hours. In two cases, the temperature (e.g.,  $-26$  and  $-27.5^{\circ}\text{C}$ ) was maintained at a level close to the mean fracture temperature ( $-30.4^{\circ}\text{C}$ ). For these cases, fracture failures were observed within three and four hours after cooling was suspended. The researchers attribute the failure to the growth of microcracks in the

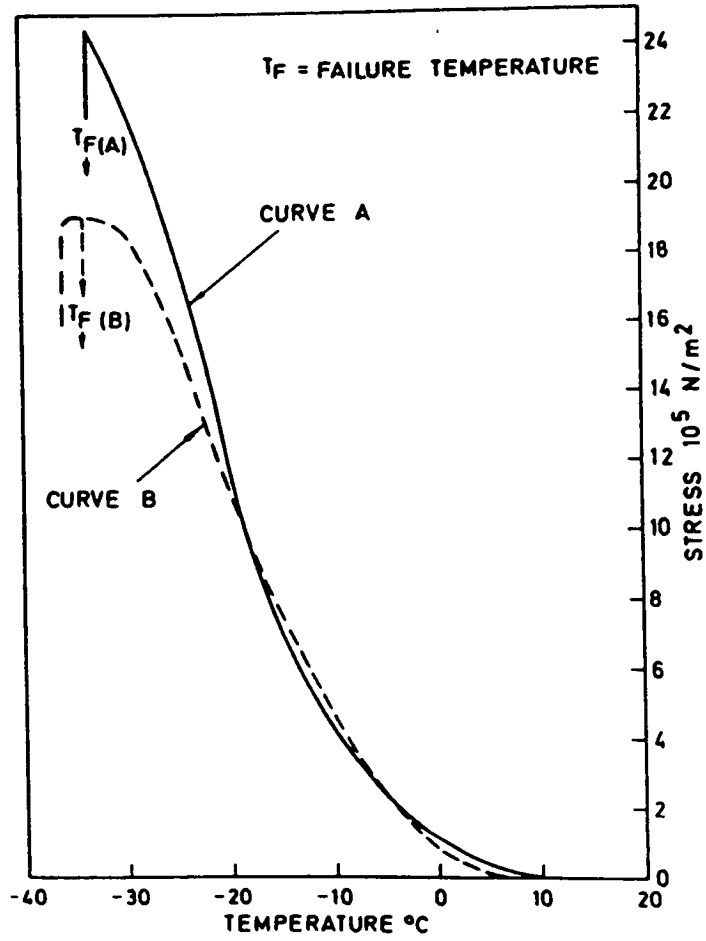


Figure 5. Stress-Temperature Relationships for Asphaltic Concretes (AC-1) (after Fabb, 1974).

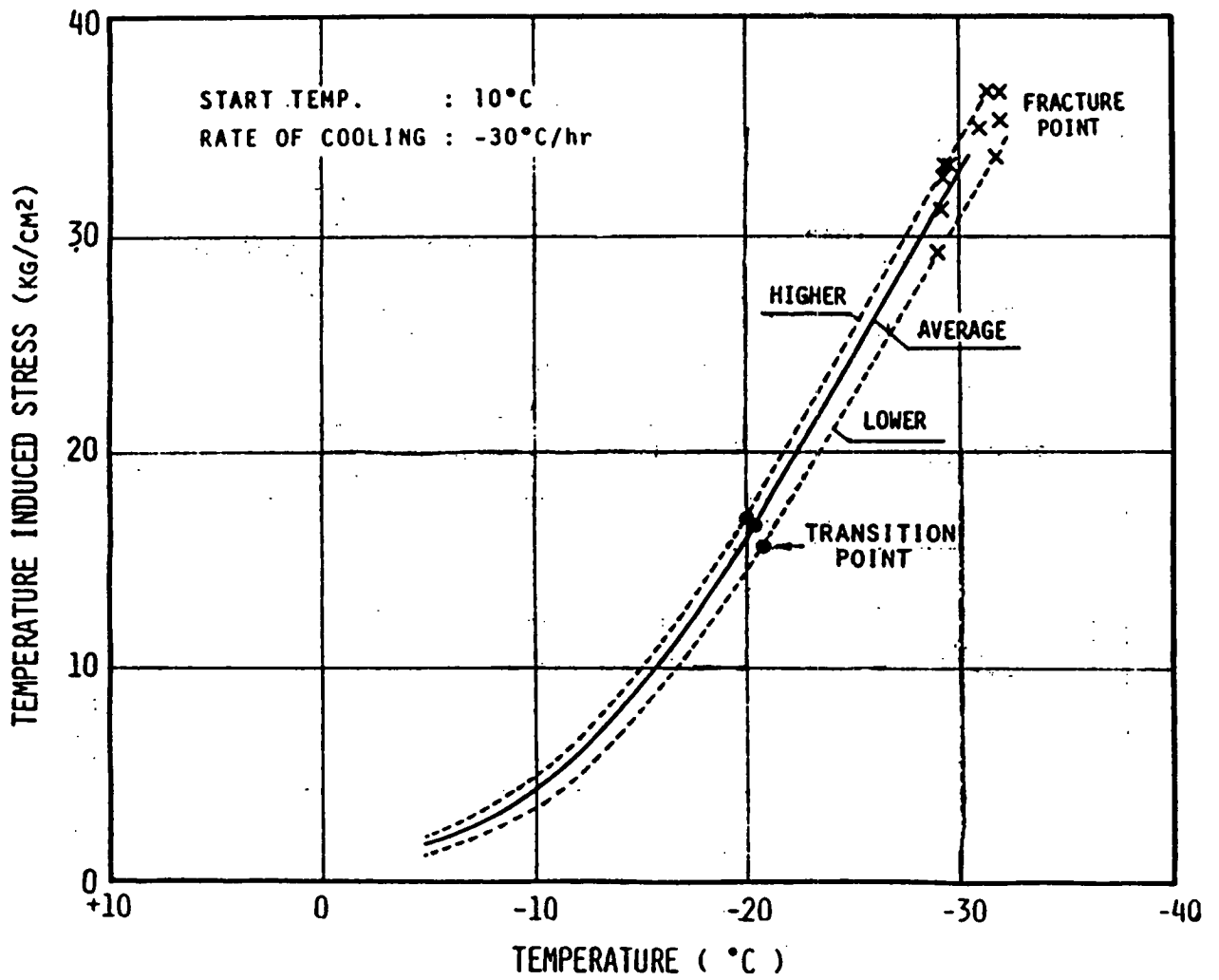


Figure 6. Thermal Fracture Tests on 10 Specimens (after Sugawara and Moriyoshi, 1984).

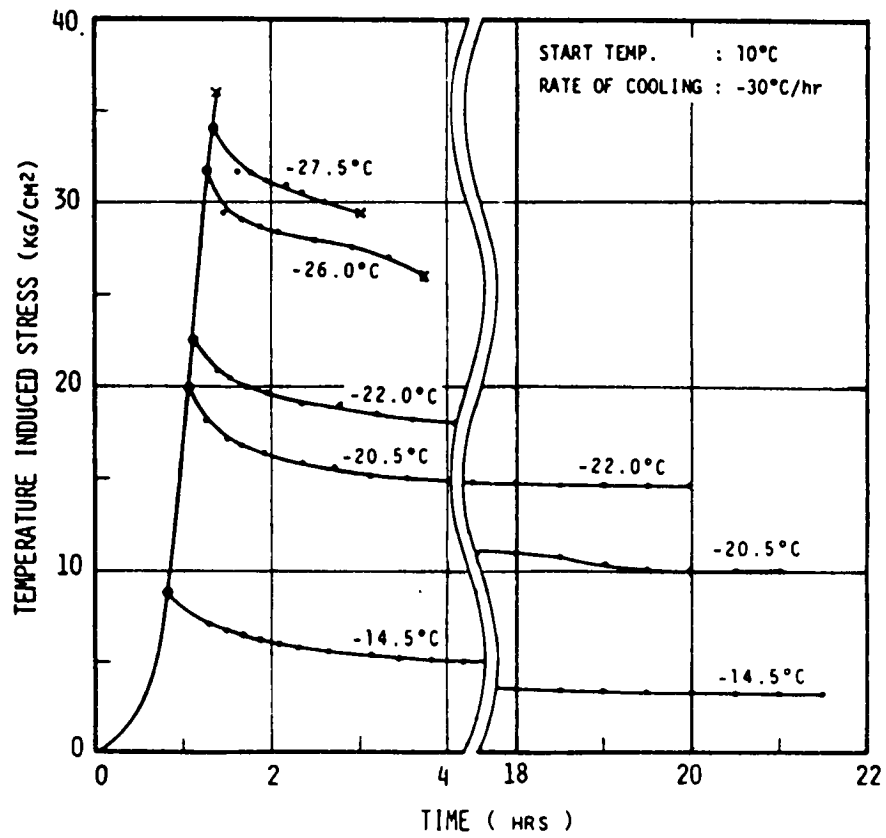


Figure 7. Change of Temperature Induced Stress at Constant Low Temperature (after Sugawara and Moriyoshi, 1984).

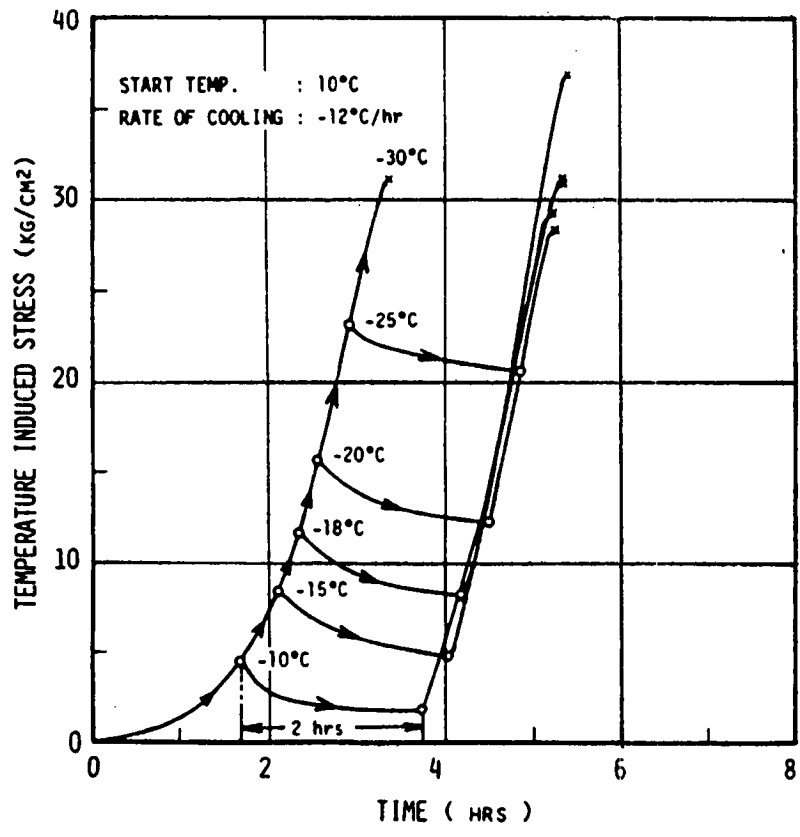


Figure 8. Change of Temperature Induced Stress at Second Cooling After 2 Hours Temperature Maintenance at Low Temperature (after Sugawara and Moriyoshi, 1984).



specimen. In other cases, fracture failures were not observed, but a marked decrease in stress occurred initially, followed by a gradual decrease with time. The results shown in Figure 8 reflect cooling down to a given temperature then maintaining the temperature for 2 hours, followed by continued cooling to fracture. The results suggest the thermal stress temperature relationship is not affected by the thermal history. The results shown in Figure 9 reflect cooling down to given temperatures of  $-15$ ,  $-20$ , and  $-25^{\circ}\text{C}$ , then raising the temperature to  $10^{\circ}\text{C}$  followed by cooling to fracture. Again, the results suggest the thermal stress temperature relationship is not affected by the thermal history.

Arand (1989) conducted an investigation to identify the relationship between aggregate gradation, viscosity of the asphalt cement, and fracture temperature. The test results were interpreted with a multiple linear regression analysis and are presented in Figure 10. The aggregate gradation is described by the exponent in the Talbot function. The asphalt cement viscosity is reflected by the ring and ball softening point temperature.

The volume of an asphalt concrete mix decreases as the temperature is decreased. The relative decrease in volume with decreasing temperature is expressed by the coefficient of thermal contraction. The average value of the volumetric thermal coefficient of contraction defined over a temperature interval  $\Delta T$  is expressed by:

$$\beta = \frac{\Delta V}{\Delta T V_0} \quad (2)$$

in which,

$$\begin{aligned} \beta &= \text{volumetric coefficient of thermal contraction} \\ V_0 &= \text{volume at some reference temperature} \end{aligned}$$

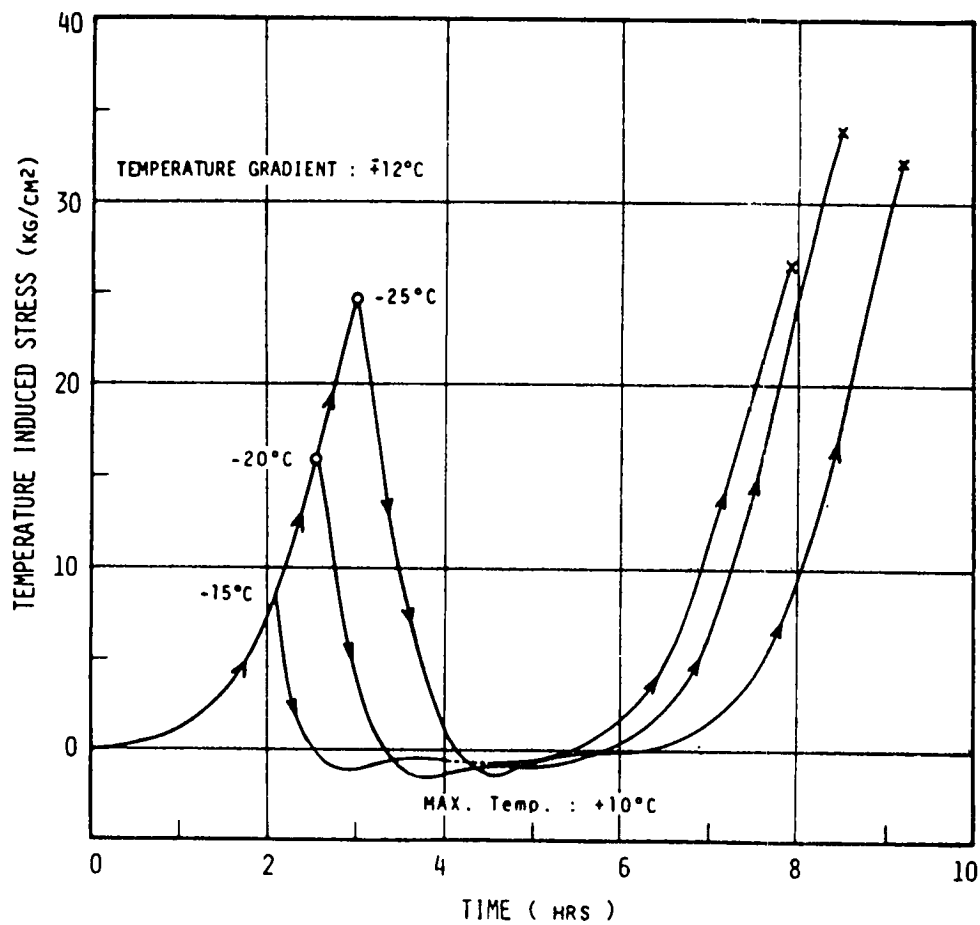


Figure 9. Change of Temperature Induced Stress Under Cyclic Temperature Change (after Sugawara and Moriyoshi, 1984).

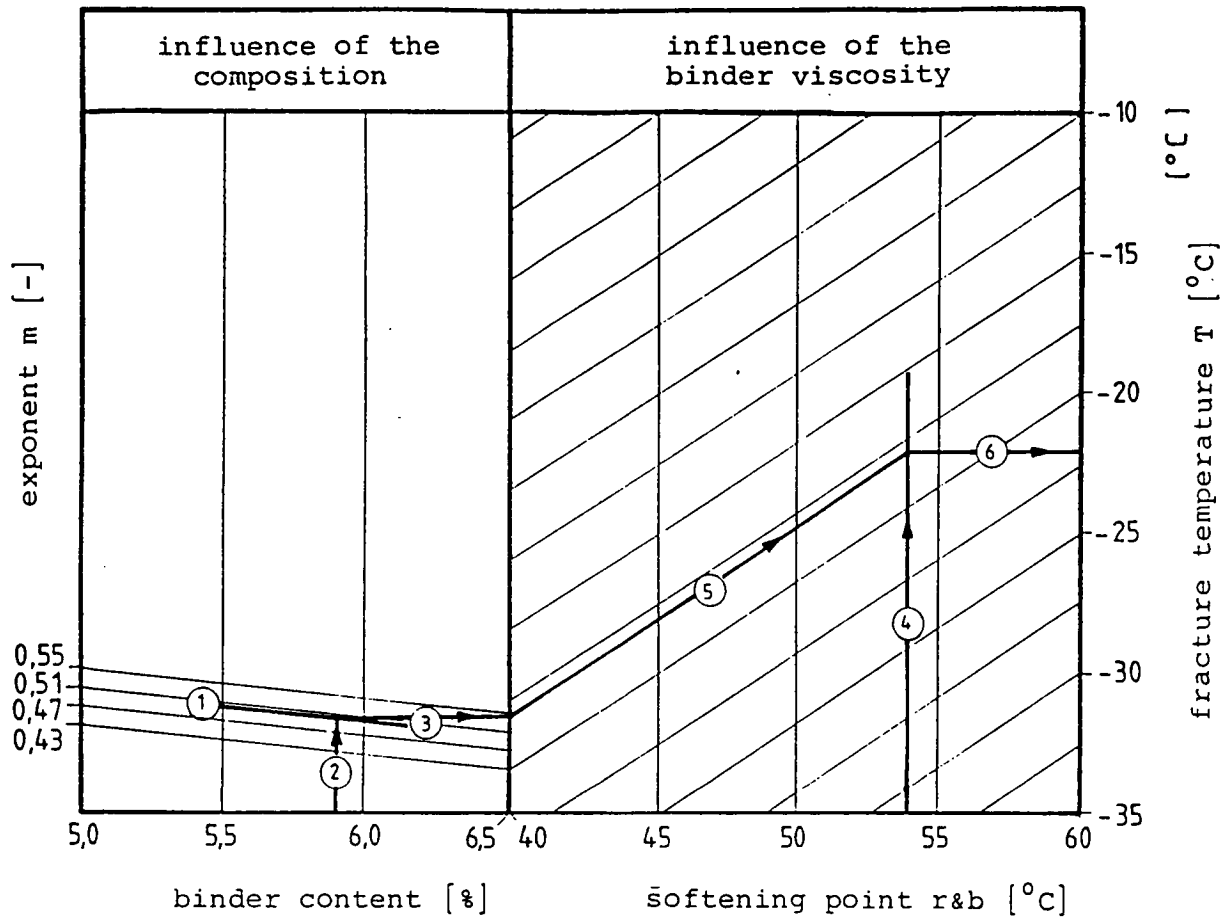


Figure 10. Fracture Temperature as a Function of Aggregate Gradation, Asphalt Cement Content, and Asphalt Viscosity (after Arand, 1989).

$\Delta V$  = change in volume because of temperature change  $\Delta T$  from reference temperature

The relative decrease in length of a material with decreasing temperature is expressed by the linear thermal coefficient of contraction

$$\alpha = \frac{\Delta L}{\Delta T L_0} \quad (3)$$

in which,

$\alpha$  = linear thermal coefficient of contraction

$L_0$  = length at some reference temperature

$\Delta L$  = change in length because of temperature change  $\Delta T$  from reference temperature

If a material exhibits the same thermal expansion in every direction, it is said to be isotropic. For an isotropic material, the linear thermal coefficient of contraction is equal to

$$\alpha = \beta/3 \quad (4)$$

Asphalt cement exhibits two coefficients of thermal contraction. These are called the *glassy* and the *fluid* coefficients. The temperature at which this change of thermal coefficient takes place is called the glass transition temperature ( $T_g$ ). For temperatures warmer than  $T_g$ , asphalt exhibits its fluid coefficient of contraction. For temperatures colder than  $T_g$ , asphalt exhibits its glassy coefficient of contraction. The physical properties of asphalt are significantly different in the fluid and glassy states. Some properties change in a nearly discontinuous manner at the glass transition temperature; other properties change gradually over a small temperature range.

The glass transition temperature may be determined by several experimental techniques, but traditionally is determined by measuring the specific volume change over a wide range of temperatures. At the glass transition

temperature, the volume-temperature curve has an abrupt change in slope as shown in Figure 11. Schmidt and Santucci (1966) investigated the  $T_g$  of 52 asphalt sources that were representative of commercial production in the United States. They reported  $T_g$  values ranging from  $-36$  to  $-15^\circ\text{C}$  with an average of  $-26^\circ\text{C}$ . Sugawara and Moriyoshi (1984) have interpreted several phenomenological observations in their research program in terms of the glass transition temperature. For example, referring to Figure 7, they note that if temperature is maintained warmer than the glass transition point, stress relaxation without fracture occurs under thermal stressing, whereas if temperature is maintained colder than the glass transition point, fracture will occur.

### **2.3 Thermal Fatigue Cracking**

Daily temperature cycles that occur throughout the year produce tensile stress cycling, which can eventually fail the asphalt concrete by fatigue. The temperature range in which thermal fatigue is considered to be important, compared to the temperature range in which low temperature contraction is considered to be important, is shown in Figure 12. The potential for fatigue failure often is evaluated by considering the ratio of applied stress to strength. The closer this ratio is to unity, the more rapidly damage accumulates. The asphalt cement characteristics are the most important factor with respect to thermal fatigue failure of a mix.

A study in which mixtures were subjected to thermal cycling until failure occurred was conducted by Sugawara and Moriyoshi (1984). Typical test results are shown in Figure 13. Fatigue type failures were observed when the minimum temperature was set close to the fracture temperature. In the harder asphalt cements, fatigue-type failures were observed at a lower number of thermal

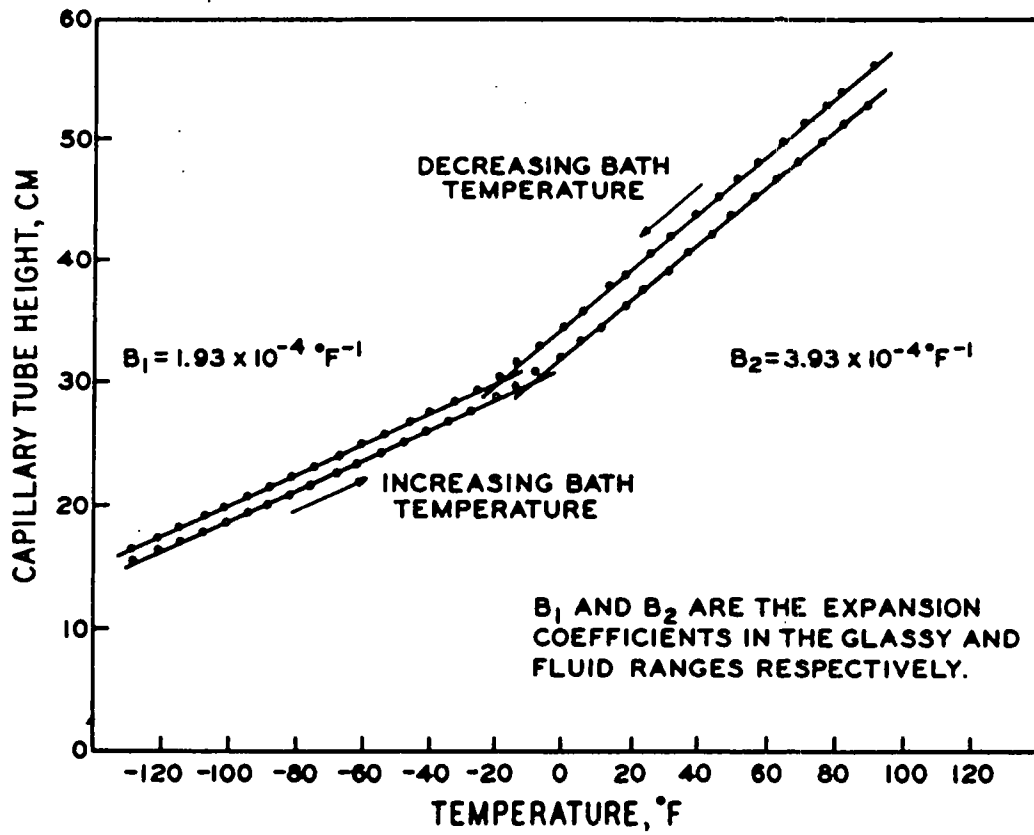


Figure 11. Typical Expansion of Asphalt with Temperature Change (after Schmidt and Santucci, 1966).

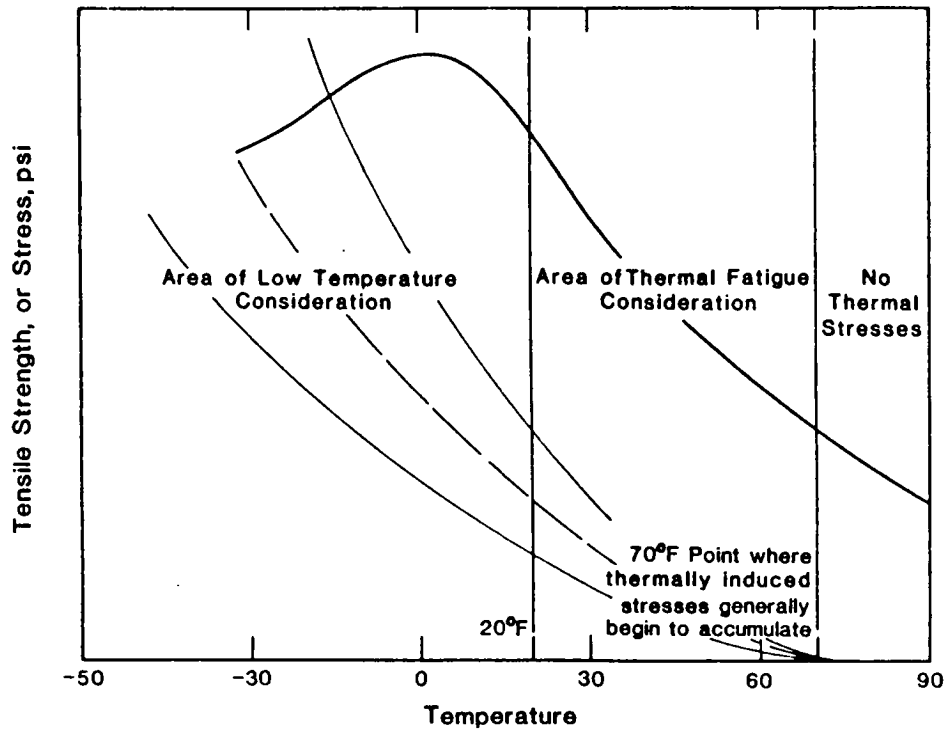


Figure 12. Temperature Ranges Associated with Different Types of Thermal Cracking (after Carpenter, 1983).

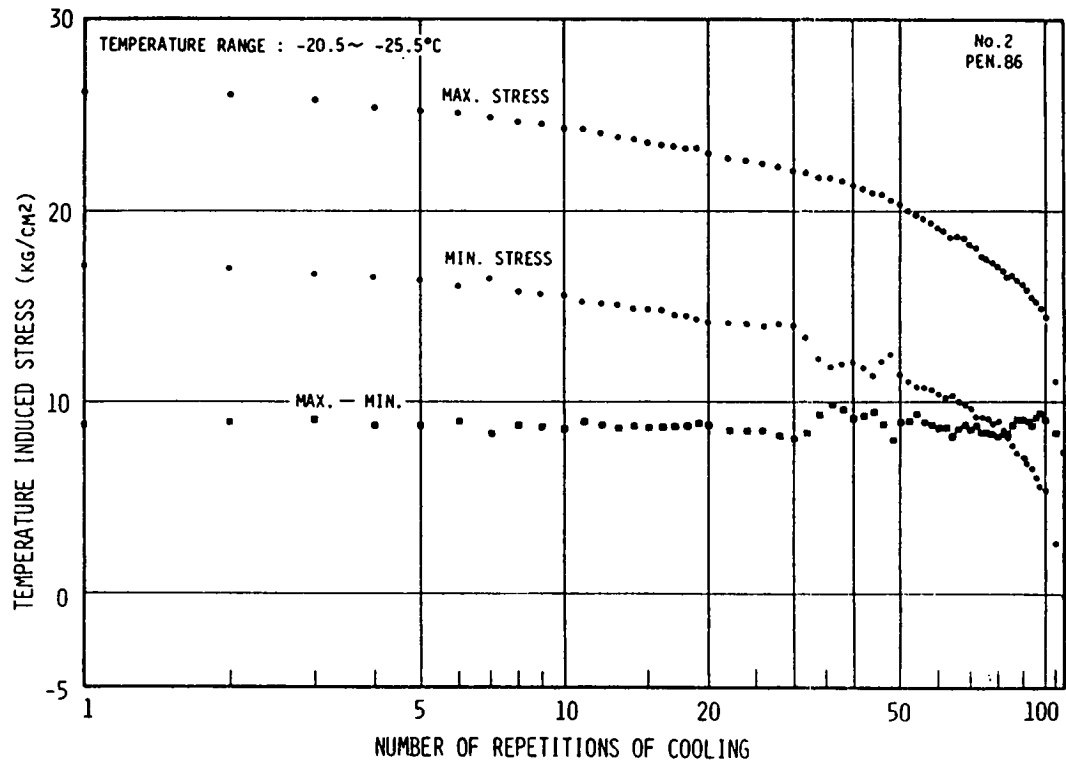


Figure 13. Change of Thermal Stress and Fracture Under 120 Repetitions of Cooling (between -20.5 and -25.5°C) (after Sugawara and Moriyoshi, 1984).



cycles compared with softer asphalt cements. The researchers note that the results obtained from the repeated cooling tests are similar to those obtained from conventional fatigue tests, but the number of repetitions to failure was much less for the thermal cycling tests because the applied cyclic stress and initial level of stress were great.

Approaches to the thermal fatigue problem, while in their infancy, may be classified as phenomenological or mechanistic. In the phenomenological approach, tests similar to those conducted by Sugawara and Moriyoshi (1984) may be used to identify the number of thermal cycles to failure. The results from a number of tests conducted at different thermal cycle magnitudes and initial temperatures would be used to arrive at a distress function that would be similar to that identified in conventional (i.e. load related) fatigue failures of asphalt concrete, namely,

$$N_f = c \left( \frac{1}{\sigma} \text{ or } \frac{1}{\epsilon} \right)^m \quad (5)$$

in which,

- $N_f$  = number of load applications to failure
- $\sigma$  = tensile stress
- $\epsilon$  = tensile strain
- $c, m$  = factors that depend on the material composition, mix properties, etc.

The phenomenological approach may provide a reasonably simple procedure to interpret thermal cycle test results. Shahin and McCullough (1974) presented a damage model for predicting temperature cracking in flexible pavements that is based on the phenomenological approach. However, the phenomenological approach has been criticized because it cannot account for crack initiation

and propagation and the subsequent redistribution of stresses within a layered system (Majidzadeh, et al., 1977).

Mahboub (1985) and Little and Mahboub (1985) note that the differentiation between crack initiation and propagation may be important in estimating thermal fatigue life. If asphalt concrete behaves in a brittle manner, as will be the case at low temperatures or rapid rates of loading, the time required to initiate the crack will constitute the major portion of the fatigue life; crack propagation will be relatively fast. Conversely, as the asphalt concrete becomes more ductile, the time needed to propagate the crack to failure represents a greater fraction of pavement fatigue life.

Majidzadeh, et al. (1976) developed a mechanistic approach based on the postulate that fatigue life can be described by a linear elastic fracture mechanics process of crack initiation, propagation, and ultimate fracture. (Only crack propagation and ultimate fracture were modeled; crack initiation was ignored.) In a recent evaluation and application of this approach, Abdulshafi and Majidzadeh (1985) identify the energy release rate,  $J_{1C}$ , as an appropriate material characterization for both elastic and elasto-plastic fracture mechanics approaches to predict fatigue life. Mahboub (1985) and Little and Mahboub (1985) used the  $J_{1C}$  parameter to investigate the low temperature fracture potential of plasticized sulfur binders used in paving mixtures. They note that the use of diametral indirect tensile strength test results to differentiate the low temperature fracture potential of plasticized sulfur binders proved to be unsatisfactory. Abdulshafi and Kalosh (1988) used the  $C^*$  line integral, another energy rate release parameter, to differentiate the performance of modified asphalt concrete mixtures with respect to load-fatigue cracking distress. They note that test methods that measured the Marshall stability, compressive strength, resilient modulus, and indirect

tensile strength could not be used to clearly differentiate the performance of the modified mixtures. Abdulshafi and Kalosh suggest the C\*-line integral also could be used to study thermal cracking of asphalt concrete mixtures. Lytton and Shanmugham (1982) have developed a mechanistic model based on fracture mechanics to predict the number of temperature cycles required to crack a pavement.

## **2.4 Summary of Factors Influencing Response**

Factors that influence low temperature and thermal fatigue cracking of pavements may be broadly categorized under (1) material, (2) environmental, and (3) pavement structure geometry. A discussion of specific factors under each of these categories follows.

### **Material Factors**

Several material factors can affect the thermal behavior of asphalt-aggregate mixtures. These include:

- 1) Asphalt Cement – There is considerable agreement that the single most important factor that affects the degree of low temperature cracking in an asphalt concrete mix is the temperature-stiffness relationship of the asphalt cement. The stiffness or consistency (i.e., viscosity or penetration) at a cold temperature and the temperature susceptibility (i.e., the range in consistency with temperature) are the most important considerations. A lower viscosity (or higher penetration) grade of asphalt cement will produce a lower rate of increase in stiffness with decreasing temperature and reduces the potential for low temperature cracking. Anderson, et al., (1989), the Committee on Characteristics of Bituminous Materi-

als (1988) and Carpenter and VanDam (1985), have conducted comprehensive studies on the relationships of asphalt cement to low temperature cracking. An annotated bibliography on the temperature susceptibility of asphalt cements recently has been published by the Transportation Research Board (1989).

- 2) Aggregate Type and Gradation – Maximum resistance to transverse cracking is associated with aggregates that have high abrasion resistance, low freeze-thaw loss and low absorption. Aggregates that possess these characteristics show little variation in low temperature strengths. Absorptive aggregates reduce low temperature strength because the asphalt cement remaining in the mixture for bonding is less than it would be in a mixture with a non-absorptive aggregate. The gradation of the aggregate used in the mix apparently has little influence on the low temperature strength, assuming the mix is designed to provide reasonable resistance to rutting.
- 3) Asphalt Cement Content – Changes in asphalt cement content, within a reasonable range about the optimum, do not have a significant influence on low temperature cracking performance of the mix. Increasing the asphalt cement content increases the coefficient of thermal contraction, but lowers the stiffness. The apparent net effect is that the thermal stress that develops is similar to the stress developed before the asphalt cement content was changed.
- 4) Air Voids Content – The degree of compaction and related air voids content and permeability are not factors that, by them-

selves, significantly influence low temperature cracking performance of the mix.

### **Environmental Factors**

Several environmental factors can affect thermal behavior. These include:

- 1) Temperature – For a given mix, the colder the pavement surface temperature the greater the incidence of thermal cracking. The pavement surface temperature is related to the ambient air temperature and wind speed. The majority of low temperature cracks apparently are initiated when the temperature decreases to a level below the glass transition temperature and is maintained at this level for a period of time.
- 2) Rate of Cooling – The greater the rate of cooling, the greater the tendency for thermal cracking. Evidence suggests that pavements may crack in the fall or spring when the pavement structure is subjected to the greatest temperature differential between day and night.
- 3) Pavement Age – The older the pavement, the greater the incidence of thermal cracking. This is associated with the increase in stiffness of the asphalt cement with age. The air void content of the mix may influence the aging characteristics of the mix. Also, with time in service, there is an increasing probability of occurrence of more extreme low temperatures as the pavement becomes older. Benson (1976), in a study of low temperature pavement cracking in Texas, proposed a generalized

model for predicting the hardening of asphalt as a function of time.

### **Pavement Structure Geometry**

Several pavement structure geometry factors can affect thermal cracking response. These include:

- 1) **Pavement Width** – Field evidence suggests that thermal cracks are more closely spaced for narrow pavements compared to wide pavements. Initial crack spacing for secondary roads 24 ft in width is approximately 100 ( $\pm$ ) ft, whereas for general aviation airports, with pavements of the order of 50–100 ft in width, the initial spacing can be greater than 150 ( $\pm$ ) ft. As the pavement ages, and secondary and tertiary cracks develop, the differences in crack spacing are not apparent.
- 2) **Pavement Thickness** – In general, the thicker the asphalt concrete layer (ACL), the lower the incidence of thermal cracking. At the Ste. Anne Test Road, increasing the thickness of the ACL from 4 to 10 in. resulted in one half the cracking frequency when all other variables were the same.
- 3) **Friction Coefficient Between the Asphalt Concrete Layer and Base Course** – The use of a prime coat on an untreated aggregate base course layer apparently reduces the incidence of low temperature cracking. This may be because of the fact that an asphalt concrete layer that is bonded perfectly to an underlying granular base has a reduced coefficient of thermal contraction owing to the lower coefficient of thermal contraction of the granular base. The gradation of the base course, particu-

larly the percentage of material finer than the No. 200 sieve, may have a minor influence on the incidence of low temperature cracking.

- 4) Subgrade Type – The frequency of low-temperature shrinkage cracking usually is greater for pavements on sand subgrades compared with cohesive soils.
- 5) Construction Flaws – Steel roller compaction of asphalt layers at high temperatures and low mix stiffness, creates transverse flaws. As the pavement cools, cracks may be initiated at these flaws, often at spacings closer than the width of a lane.

## 2.5 Regression Equations to Predict Thermal Cracking

Based on an analysis of data from 26 airports in Canada, Haas, et al., (1987) established a regression equation to predict the average transverse crack spacing in a pavement structure, as follows:

$$\text{TRANCRACK} = 218 + 1.28 \text{ ACTHICK} + 2.52 \text{ MINTEMP} + 30 \text{ PVN} - 60 \text{ COEFFX} \quad (6)$$

$$r^2 = 0.70$$

in which,

TRANCRACK	=	Transverse crack average spacing in meters
MINTEMP	=	Minimum temperature recorded on site in °C
PVN	=	MacLeod's Pen Vis Number (asphalt cement temperature susceptibility, which is dimensionless)
COEFFX	=	Coefficient of thermal contraction in mm/1000 mm/°C
ACTHICK	=	Thickness of the asphalt concrete layer in centimeters

Additional regression equations were developed for situations in which: a) the PVN were not available, and/or b) the designer does not choose to use the PVN value, and/or c) the designer wishes to use the mix temperature susceptibility

(in terms of stiffness modulus increase from 0°C to -17°C) instead of PVN, and/or d) the coefficient of thermal contraction is not available.

The PVN in equation (6), which may be determined from the penetration at 77°F and the kinematic viscosity at 275°F, is an indicator of temperature susceptibility of the asphalt cement (McLeod, 1972, 1987). As the PVN decreases, for a given grade of asphalt, the temperature susceptibility increases. Consequently, as the PVN decreases, the average crack spacing increases. Further, crack spacing increases with pavement age and minimum temperature, but decreases with pavement thickness. These trends are expected based on the observations of other researchers.

Fromm and Phang (1972) conducted field surveys of 33 pavement locations in Ontario to assess the severity of thermal cracking. They developed the crack index (CI) as a measure of cracking severity, as follows:

CI = The sum of numbers of multiple and full-transverse cracks with one half the number of half-transverse cracks occurring in a 500 ft stretch of two-lane pavement.

The types of transverse cracks used to establish the CI are shown in Figure 14. Smaller transverse cracks were disregarded in the calculation of the CI.

Extensive field sampling and laboratory testing of pavement structure materials at the 33 locations also was conducted. Based on a consideration of this data, the following regression equation was established:.

$$\begin{aligned} \text{CI} = & 52.22x_1 + 0.0007093x_2 + 0.4529x_3 - 1.348x_4 + 0.4687x_5 \\ & - 0.07903x_6 - 0.4887x_7 - 0.1258x_8 - 0.1961x_9 \end{aligned} \quad (7)$$

Multiple Correlation Coefficient  $r = 0.6357$



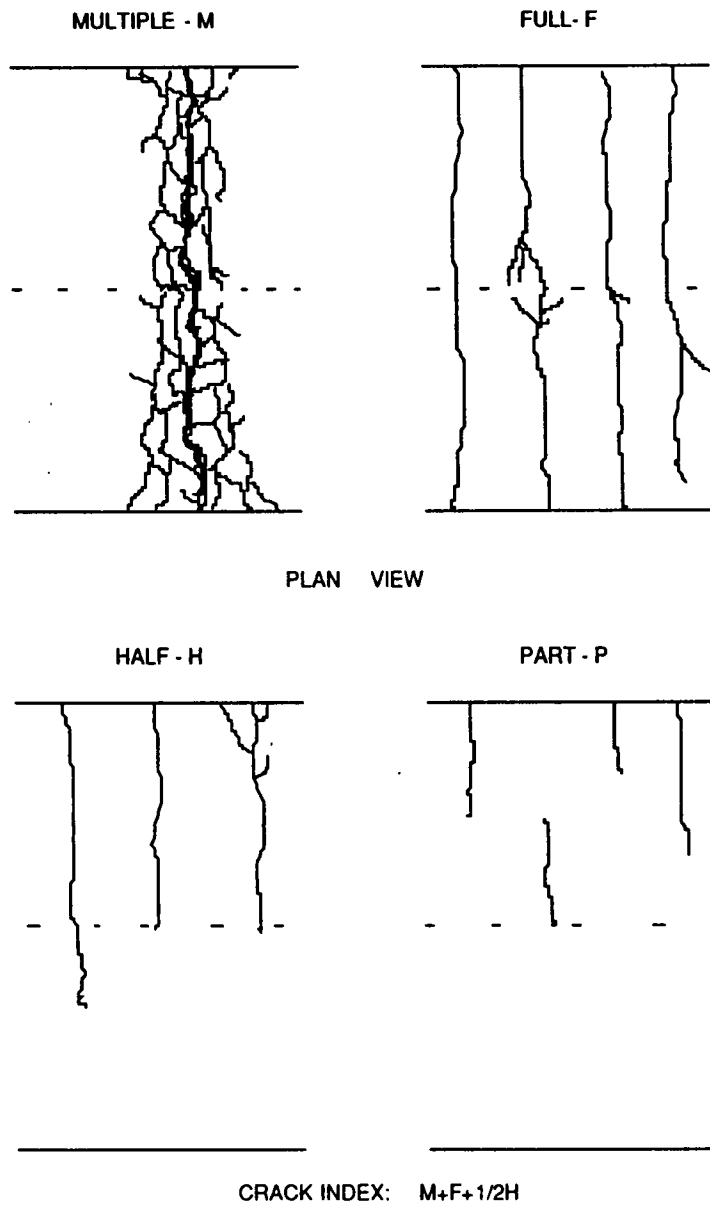


Figure 14. Types of Transverse Cracking (after Fromm and Phang, 1972).

in which,

- $x_1$  = viscosity ratio, visc. 60°F megapoises/visc. 275°F centistokes
- $x_2$  = freezing index, degree days
- $x_3$  = critical temperature, °F
- $x_4$  = pavement air voids, % vol.
- $x_5$  = stripping rating
- $x_6$  = recovered asphalt pen. at 77°F, dmm
- $x_7$  = asphaltenes, % wt.
- $x_8$  = granular base, pass 200, % wt.
- $x_9$  = asphalt concrete, pass 200, % wt.

The paving contracts then were divided into northern and southern groups based on the grade of asphalt used. Penetrations less than 110 were placed in the southern group (85–100 asphalts), and penetrations equal to or greater than 110 were placed in the northern group (150–200 asphalts). Based on this division, two additional regression equations were established (but are not presented herein).

The viscosity ratio in equation (7) is an approximate indicator of temperature susceptibility. A larger ratio indicates a stiffer consistency at low temperatures. The greater the critical temperature (i.e., the temperature at which the viscous flow of the asphalt concrete in one hour is exceeded by the thermal contraction in the specimen), the greater the potential for cracking. The variables that relate to other characteristics of the mix, such as air voids, recovered asphalt penetration, asphaltenes, and percent fines, appear to be modelled correctly regarding their influence on thermal cracking. Also, as the fines content of the base course increases, the potential for cracking decreases. The model does not take into account the age of the pavement or the thickness of the surface layer, but it does suggest the higher

the moisture susceptibility of the mix (i.e., stripping rating), the greater the potential for cracking.

### **3.0 DESCRIPTION OF TEST SYSTEMS AND METHODS**

A number of test methods have been used to study the phenomena of low temperature cracking in asphalt concrete mixes. The methods also have been used to provide input parameters to thermal cracking models. A discussion of the test methods follows.

#### **3.1 Indirect Diametral Tension Test**

##### **Description**

According to Hadipour and Anderson (1988), the test is conducted by loading a 4 in. diameter by 2.5 in. thick cylindrical asphalt concrete specimen through loading strips placed across a diameter. The specimen is within a controlled temperature chamber. As the specimen is compressed at a deformation rate of 1.5 mm/min., a relatively uniform tensile stress develops perpendicular to and along the vertical diametral plane of the specimen that, if the vertical load is increased, ultimately causes the specimen to fail by splitting along its vertical diameter. The applied compressive load and the vertical and horizontal deformations are monitored through a load cell and linear variable differential transformers (LVDT), respectively. The output signals from the load cell and the LVDTs are recorded on a computerized data acquisition system. A schematic of the test system is shown in Figure 15.

Von Quintus, et al., (1988) noted that tensile strengths determined with the indirect diametral tension test provided input data to thermal cracking models that they used to rank asphalt mixtures under the AAMAS project. The mixture strength was measured on age-hardened specimens using an environmental aging simulation. A loading rate of 0.05 in. per min. was used to represent the thermal loads on the pavement.

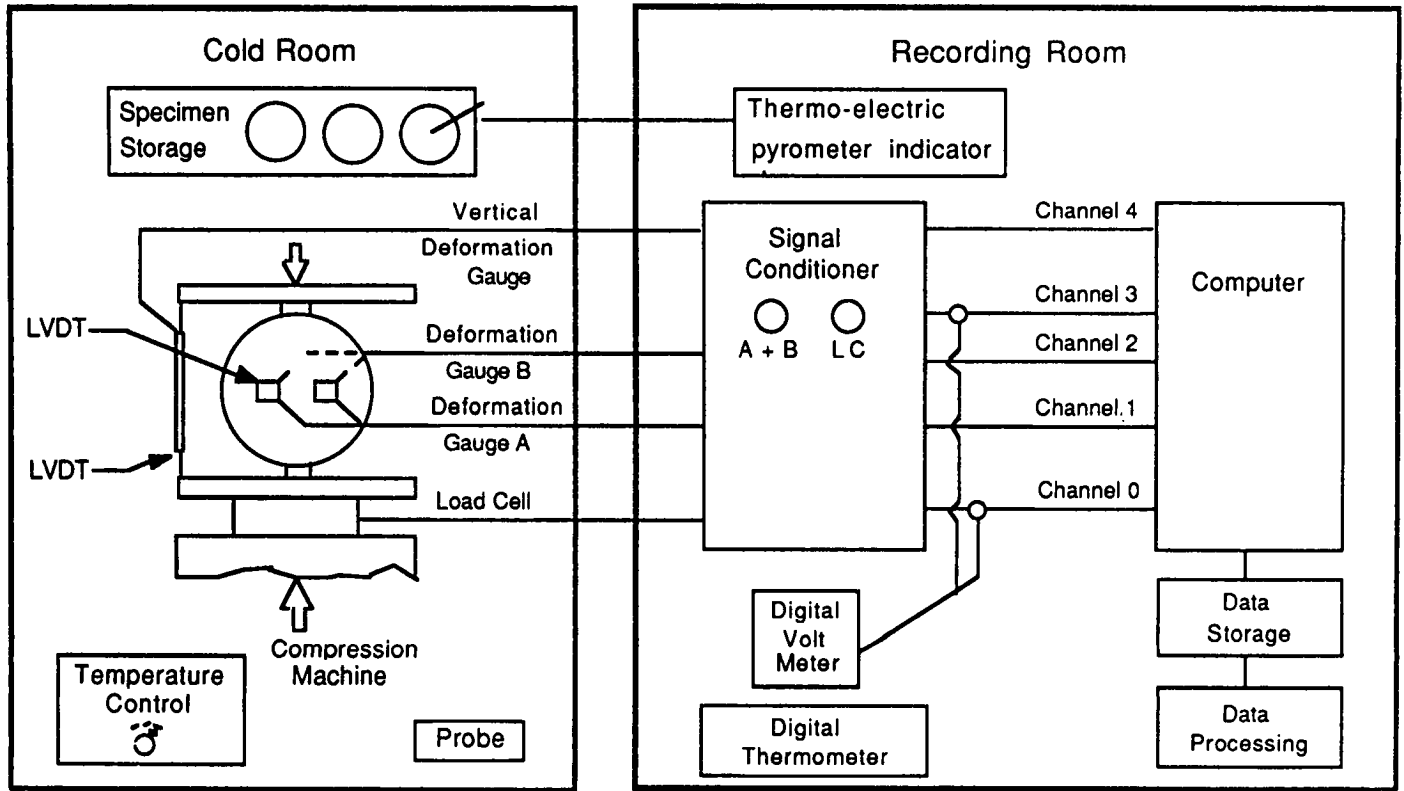


Figure 15. Schematic of Diametral Indirect Tension Test Equipment (after Anderson and Leung, 1987).

Alternatively, the test may be conducted using dynamic loads that do not produce failure (reference: ASTM D-4123). The stress-strain response is represented by the resilient modulus determined under the applied dynamic load.

### **Test Condition Parameters**

Temperature, specimen geometry and volume, and deformation or load rate.

### **Properties Measured**

Tensile stress/strain characteristics; tensile strength.

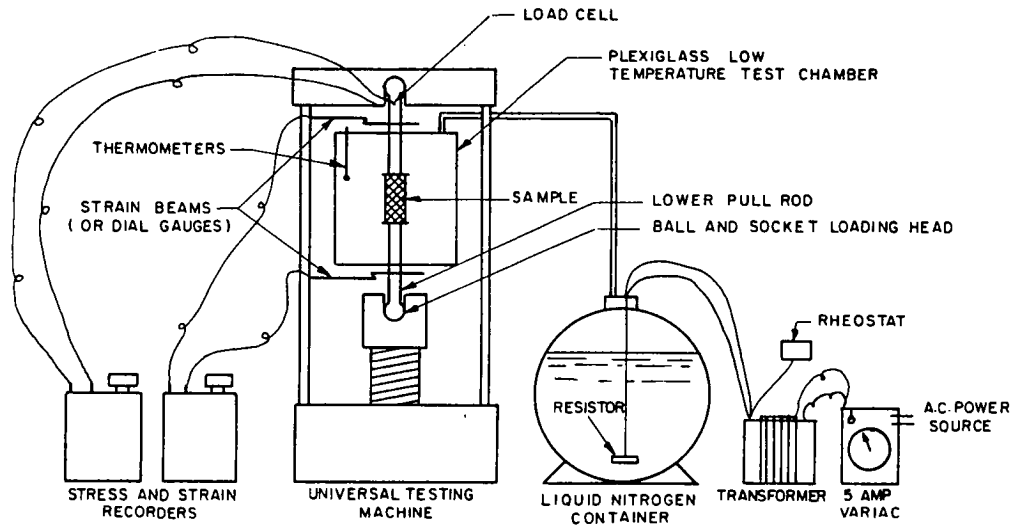
### **Agency/Institutional References**

University of Florida, Ruth (1977); University of Alberta, Hadipour and Anderson (1988); Anderson and Leung (1987).

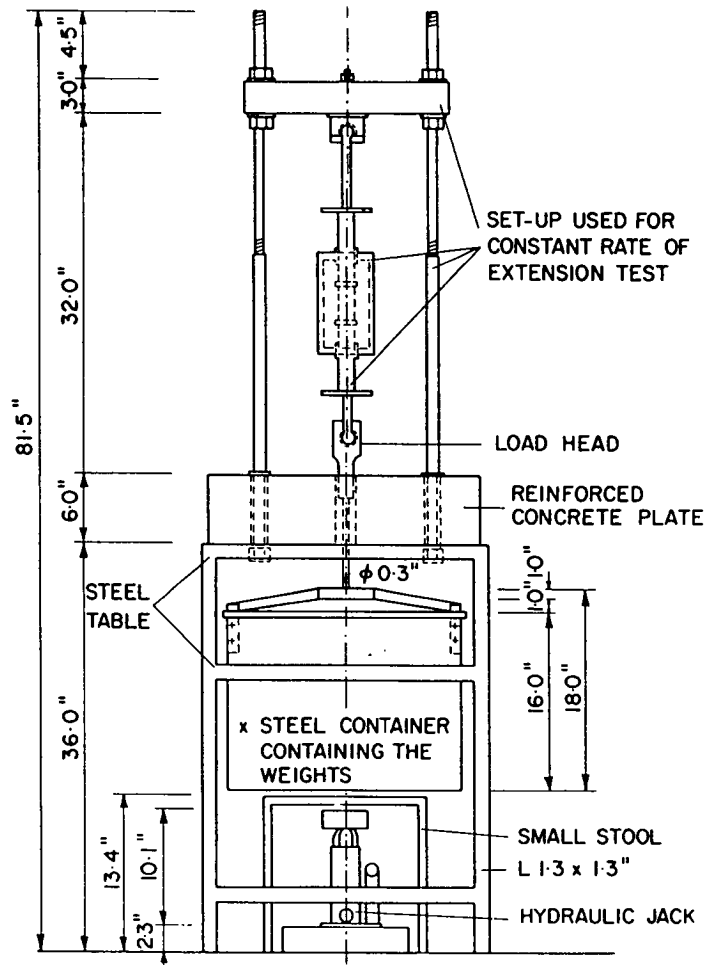
## **3.2 Direct Tension - Constant Rate of Extension**

### **Description**

Haas (1973) subjected a rectangular beam specimen to a tensile load at a control temperature and a constant rate of extension. The variables recorded during the test are (1) extension of the specimen, (2) temperature, (3) load, and (4) time. The test system is shown in Figure 16. It consists of the following components: (1) a universal testing frame, (2) an environmental chamber, (3) an extension measuring apparatus, (4) a load cell, (5) a piston loading rod specifically noted because it is fabricated from a material with a low coefficient of heat transfer and a low coefficient of thermal expansion and contraction. The test specimens are 1.5 × 1.5 × 4 in. The ends of the test specimens are epoxied to the cap and base plates. The most recent version (1988) of the test system includes a universal testing machine, which



a) Overall Test System



b) Constant Rate of Extension and Creep Load Frame

Figure 16. Schematic of Direct Tension and Creep Load Test Systems (after Haas, 1973).

can provide extremely slow rates of extension, located in a cold room with the capacity to test down to  $-40^{\circ}\text{C}$ . Rates of extension from  $2.5 \times 10^{-3}$  to  $12 \times 10^{-3}$  mm/min. are commonly used.

### **Test Condition Parameters**

Temperature, specimen geometry and volume, and deformation or load rate.

### **Properties Measured**

Tensile stress/strain characteristics; tensile strength.

### **Agency/Institutional References**

University of Waterloo, Haas (1973); Asphalt Institute, Kallas (1982); Technical University of Braunschweig, Germany, Arand (1987).

## **3.3 Tensile Creep Test**

### **Description**

Haas (1973) also conducted tensile creep tests with the apparatus shown in Figure 16, while Fromm and Phang (1972) used the apparatus shown in Figure 17. A creep test is conducted by applying a constant load to the specimen and recording the resulting deformation with time. The specimen is maintained at a constant temperature by placing a small test chamber around the specimen, or by placing the entire test frame in a cold room. For creep testing, the definition of modulus of creep deformation assumes an instantaneous application of load. The hydraulic jack shown in Figure 16 initially is used to support the weights prior to load application. When the jack is released, the load is applied nearly instantaneously to the specimen. The test specimens are  $1.5 \times 1.5 \times 4$  in. A load level of approximately 500 lbs is used at temperatures below  $-18^{\circ}\text{C}$  to achieve a time of loading greater than two hours.



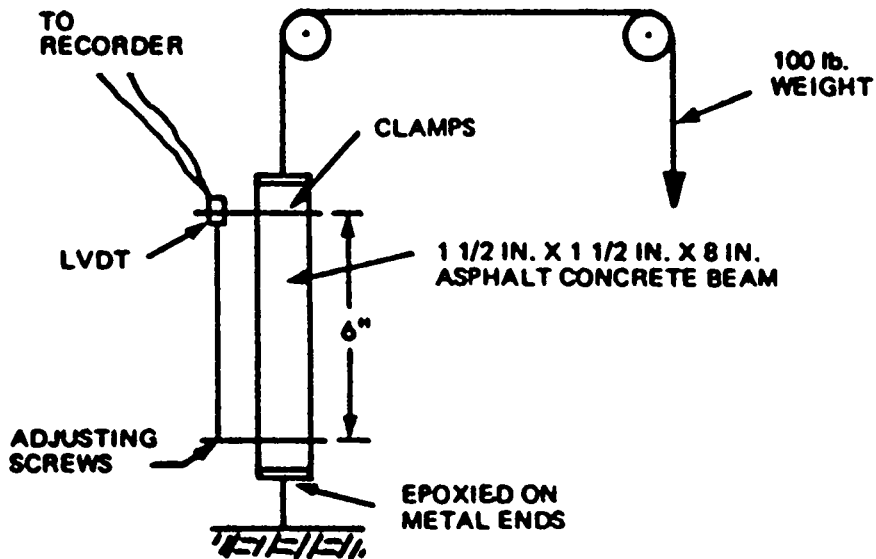


Figure 17. Apparatus for Measuring Creep Deformation Under Constant Tensile Stress (after Fromm and Phang, 1972).

### **Test Condition Parameters**

Temperature, specimen geometry and volume, and load levels.

### **Properties Measured**

Tensile stress/strain characteristics; tensile strength.

### **Agency/Institutional References**

University of Waterloo, Haas (1973); Ontario DOT, Fromm and Phang (1972).

## **3.4 Flexural Bending Test**

### **Description**

Busby and Rader (1972) determined the stiffness modulus ( $S_f$ ) and modulus of rupture ( $S_r$ ) of asphalt concrete at cold temperatures using a three-point loading test of a  $3\frac{1}{4} \times 3\frac{1}{2} \times 15$  in. beam. The stiffness modulus may be determined from

$$S_f = \frac{\delta P \cdot L^3}{48 \cdot \delta f \cdot I} \quad (8)$$

in which,

$\delta P$  = change in load applied, lb.,

$L$  = span in inches

$\delta f$  = deflection corresponding to  $P$  in inches

$I$  = moment of inertia, in.<sup>4</sup>.

The modulus of rupture, which is equivalent to the tensile strength, is determined by:

$$S_r = \frac{M \cdot c}{I} \quad (9)$$

in which,

M = moment at failure, in. lb.

c = one-half depth of beam, in.

I = moment of inertia, in.<sup>4</sup>.

The beams were tested in flexure with a universal testing machine. A relatively slow rate of loading arbitrarily was chosen to approach thermal induced stresses rather than traffic related stresses. A rate of 0.02 in. per min. was selected as a compromise between the extremes of other investigations and represents the slowest rate compatible with control equipment available to Busby and Rader.

Asphalt concrete beams were tested in flexure at  $-35^{\circ}\text{F}$ ,  $-5^{\circ}\text{F}$ , and  $+25^{\circ}\text{F}$ . The beams were placed in a freezer for a minimum of 24 hours for  $-5^{\circ}\text{F}$  and  $+25^{\circ}\text{F}$  and for a minimum of 48 hours for the  $-35^{\circ}\text{F}$  test temperatures. The beams could be at room temperature for almost 5 minutes before the temperature increased enough to affect the test results. However, to minimize the temperature change in the beam, an insulated box was constructed of styrofoam. The insulating box had shelves on which dry ice was placed to keep the temperature of the box as low as possible. The box was placed around the load frame for the duration of a test.

Sugawara, et al., (1982) conducted 3-point beam tests on  $2.5 \times 2.5 \times 25$  cm specimens. Rates of strain were from  $1 \times 10^{-4}$  to 1.9/sec and test temperatures were from  $-20$  to  $30^{\circ}\text{C}$ .

### **Test Condition Parameters**

Temperature, specimen geometry and volume, and deformation or load rate.

### **Properties Measured**

Tensile stress/strain characteristics; tensile strength.

## **Agency/Institutional References**

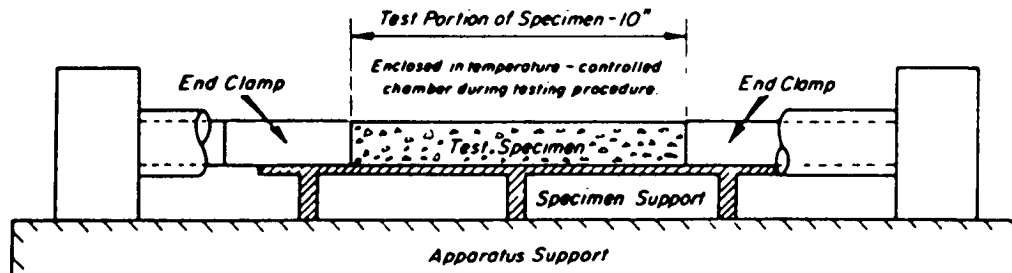
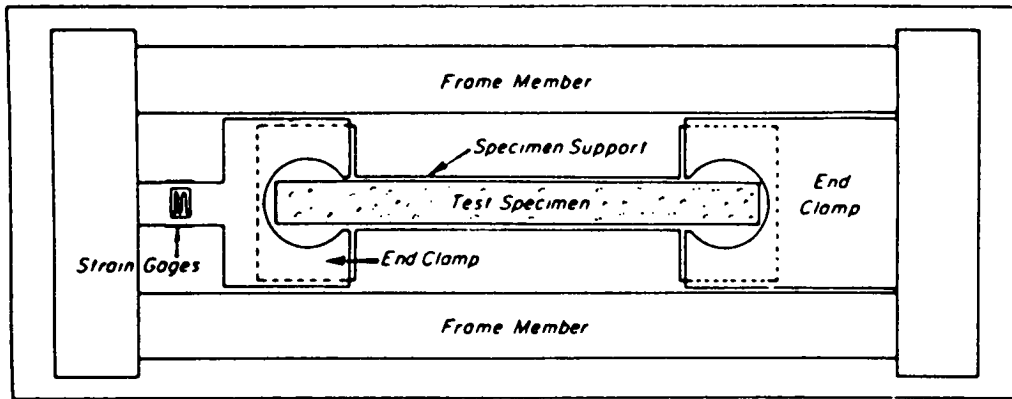
University of Wisconsin, Busby and Rader (1972); Hokkaido University, Japan, Sugawara, et al. (1982).

### **3.5 Thermal Stress Restrained Specimen Test**

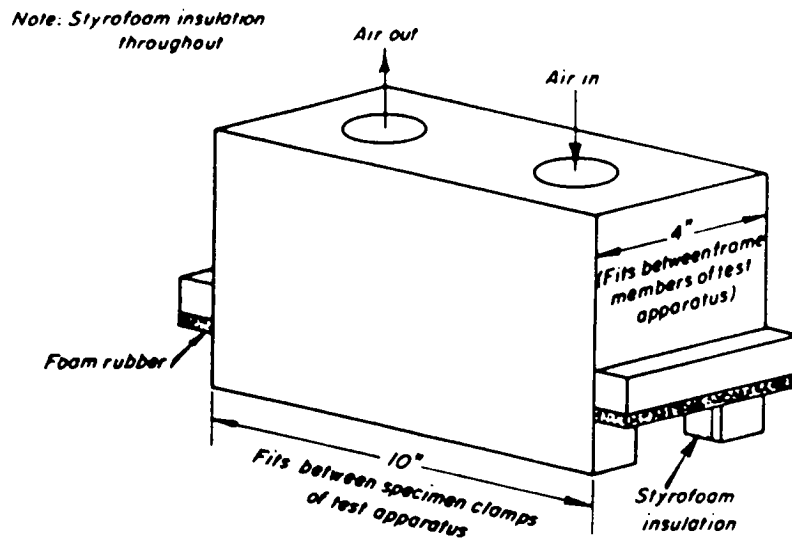
#### **Description**

Monismith, et al., (1965) conducted thermal stress tests using sawed specimens  $1 \times 1 \times 12$  in., which were placed in the invar frame shown schematically in Figure 18. The apparatus is comparatively rigid and is thus believed to be capable of restraining any deformation that may develop in the asphalt concrete because of due to temperature change. The frame is surrounded by a constant temperature cabinet to further minimize deformations. To subject the asphalt concrete specimens to temperature changes, a small cabinet is placed inside the larger chamber noted above, encompassing 10 in. of the specimen, as indicated in Figure 18. This small cabinet is connected to an external heat source, which is capable of providing the required temperature variations around the test specimen.

The test procedure reported by Monismith, et al., is as follows: 1) a specimen is placed in the invar frame with its ends inside the end clamps; 2) the temperature-controlled cabinet is placed over the specimen and the constant temperature cabinet over the entire test frame; 3) the temperature in the inner cabinet is raised to the starting test temperature of about  $140^{\circ}\text{F}$  to allow the specimen to expand freely before being clamped in position to the frame; 4) at the same time, the temperature in the outer (larger) cabinet is brought to a constant value of  $100^{\circ}\text{F}$  to allow the test frame to reach equilibrium; 5) after 4 hours at these temperatures, the outer cabinet is removed momentarily to allow the specimen ends, which project beyond the inner cabinet, to be fixed. The ends are fixed in the end clamps with an epoxy-resin



a) Thermal Stress Apparatus



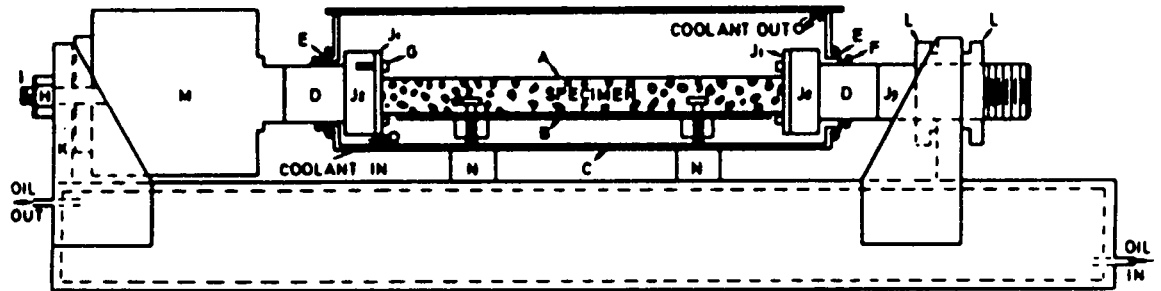
b) Controlled Temperature Cabinet for Thermal Stress Experiments

Figure 18. Schematic of Thermal Stress Restrained Specimen Test (after Monismith, et al., 1965).

compound. The resin is allowed to cure overnight while the temperatures of both the inner and the outer cabinets are held constant; 6) a test is then conducted by lowering the temperature in the small inner cabinet at any desired constant rate, while recording load and temperature. Automatic cycling in the temperature range 140°F. to 10°F. is possible for any number of cycles.

Fabb (1974) and Sugawara and Moriyoshi (1984) used different versions of the apparatus employed by Monismith, et al. The apparatus used by Fabb is shown in Figure 19. The test specimen (A), 25 × 25 × 300 mm, is supported on a stand (B) inside a brass bath (C). It is secured in the apparatus via circular Invar plates ( $J_1$ ), 5 mm thick and 63.5 mm diameter, that are fixed to each end of the specimen using special epoxy cement. These plates are fastened, by high tensile steel bolts, to tapped Invar blocks ( $J_2$ ), 20 mm thick, that are in turn permanently cemented to quartz rods (D), 44 mm long and 40 mm diameter, that pass to the outside of the bath through flexible silicone rubber diaphragms (E).

Outside the bath, one quartz rod is cemented to another Invar rod ( $J_3$ ) that is threaded and which passes through a bushed hole in the steel frame (K). It is secured by brass handwheels (L). A fine thread is used on the rod and handwheels that facilitates clamping the system together without significantly stretching or compressing the specimen. The other quartz rod is cemented to an Invar spigot that screws into the load cell (M). The load cell is securely attached to the frame by a threaded spigot (I) and a steel dowel (not shown). The base of the frame is hollow and completely enclosed. It is maintained at 25°C by oil pumped from a constant temperature bath. The bath is supported on the frame by Tufnol blocks (N) and is insulated by expanded polystyrene and polyurethane foam cladding. The lid of the bath is removable to allow insertion and removal of the specimens.



- |   |                         |   |                  |
|---|-------------------------|---|------------------|
| A | TEST SPECIMEN           | H | NUT              |
| B | SPECIMEN SUPPORT        | I | THREADED SPIGOT  |
| C | COOLING BATH            | J | INVAR COMPONENTS |
| D | QUARTZ RODS             | K | STEEL FRAME      |
| E | SEALS (SILICONE RUBBER) | L | BRASS HANDWHEELS |
| F | O RINGS                 | M | LOAD CELL        |
| G | SCREWS                  | N | BATH SUPPORTS    |

Figure 19. Schematic of Thermal Stress Restrained Specimen Test (after Fabb, 1974).

Carpenter (1983) recommended the test system shown in Figure 20. The invar steel load frame is designed to be placed in a conventional chest-type temperature cabinet. The cabinet is capable of meeting the standard temperature drop rates of 3–20°C/hr and also can achieve low temperatures to –50°C. The load frame is modularized to allow 3 × 3 × 12 in. specimens to be epoxied to aluminum plates before testing and to be stored until needed. The signal conditioning for the various displacement transducers and load cells that are used to monitor the response of the specimen are kept outside the cabinet. The LVDTs are mounted at the start of the test to determine the coefficient of thermal contraction and remain on the specimen throughout the test program. As the specimen is cooled, the deformation is noted, and the coefficient of thermal contraction may be calculated. The system, as it presently exists at USA CRREL, is slightly different than that shown in Figure 20 and is shown in Figure 21.

Arand (1989) has developed a thermal stress restrained-specimen test system with a stiff load frame, displacement transducers to measure the length of a specimen, and a step motor to hold the specimen at constant length during the conduct of a test. The step motor works in connection with a gear drive to hold the specimen at a length controllable to  $10^{-5}$  mm. The overall system is controlled with a personal computer. The equipment allows monotonic cooling tests to be conducted as well as relaxation tests and cyclic temperature tests. The equipment appears to be the best that currently is available in the highway-engineering research community.

Cooling rates from 5 to 30°C/hr have been used by researchers using the test systems described above. Based on a study of weather records in Canada, field temperature drops exceeding 5°C/hr are not common and may not occur at all (Fromm, 1974).



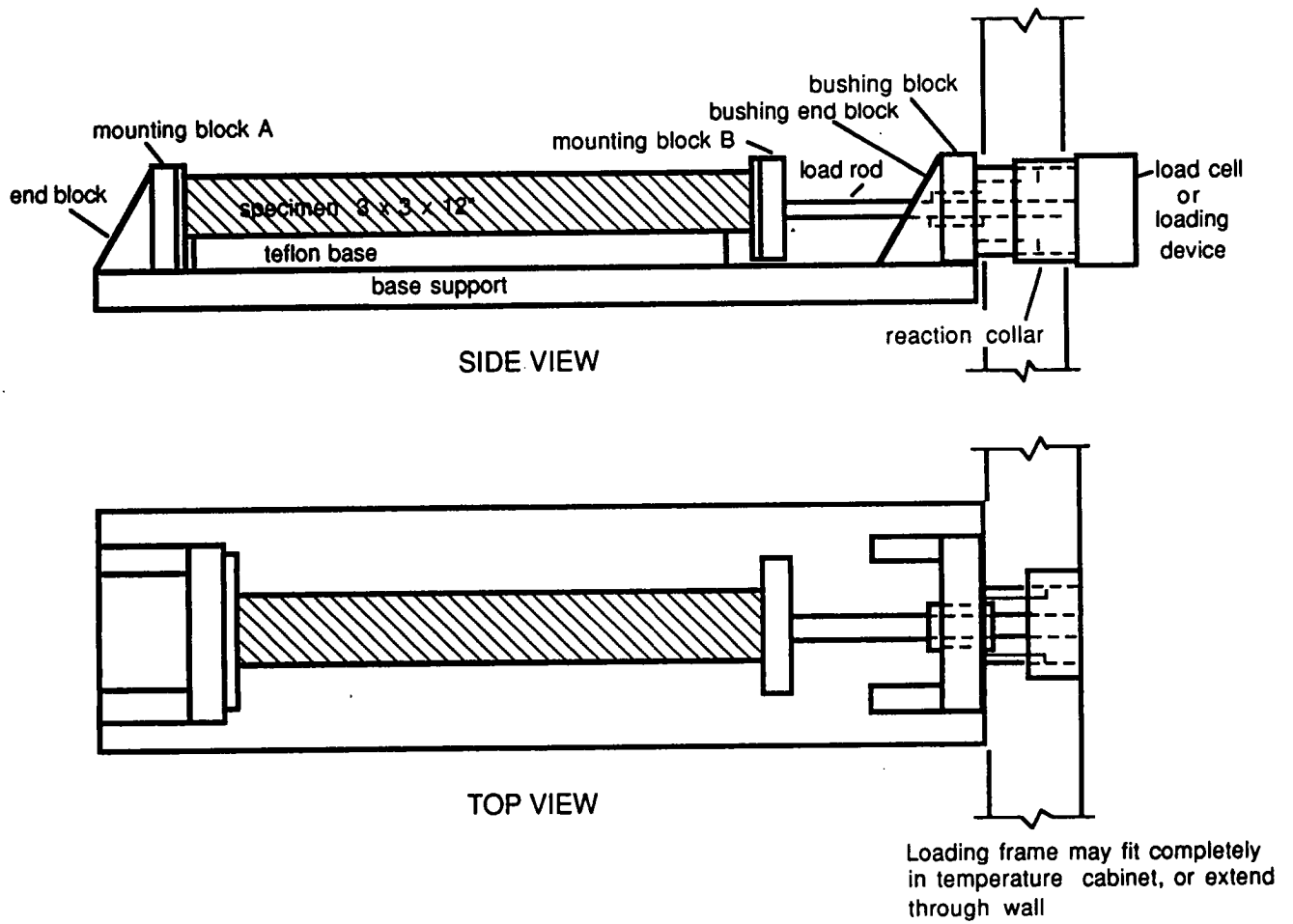


Figure 20. Schematic of Thermal Stress Restrained Specimen Test System (after Carpenter, 1983).

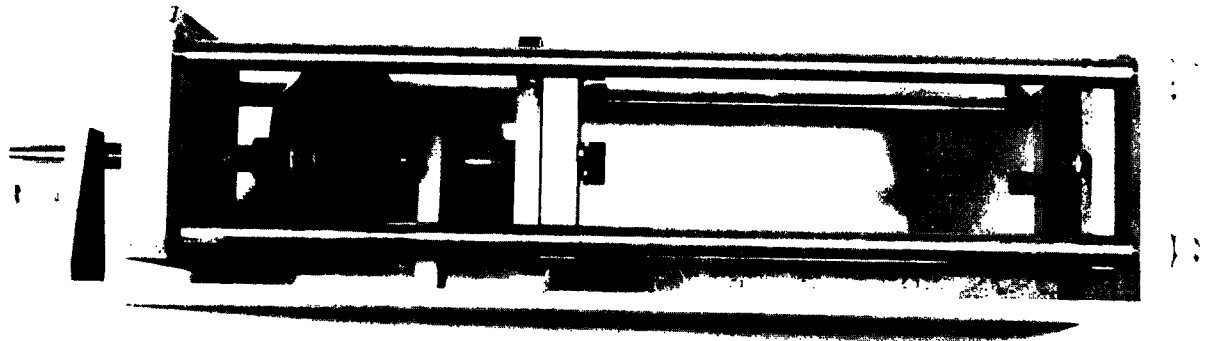
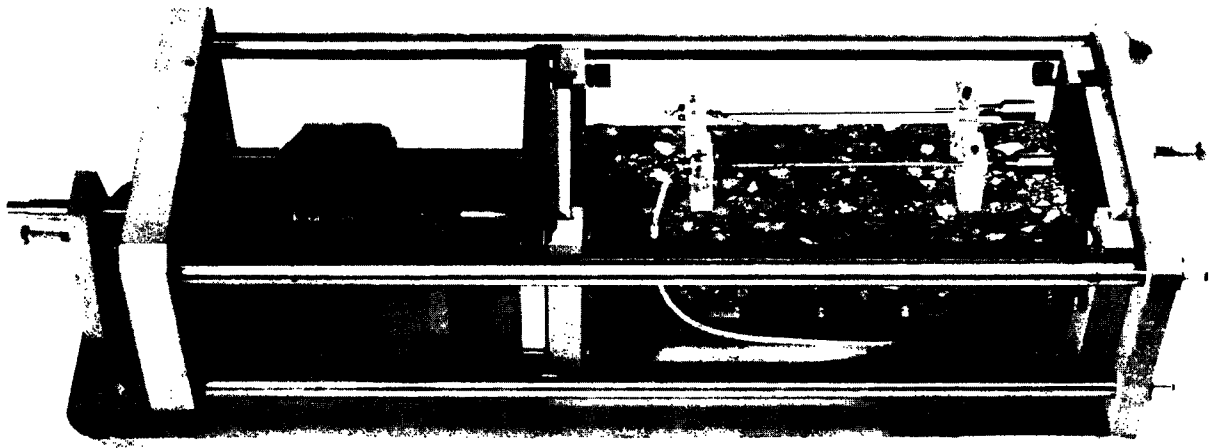


Figure 21. USA CRREL Thermal Stress Restrained Specimen Test (after Janoo, 1989).

## **Test Condition Parameters**

Specimen geometry and volume, number of thermal cycles, and rate of cooling.

## **Properties Measured**

Low temperature thermal stress characteristics; tensile/thermal fatigue strength; fracture temperature, under conditions of one or more thermal cycles.

## **Agency/Institutional References**

University of California–Berkeley, Monismith, et al., (1965); British Petroleum, Fabb (1974); Hokkaido University, Japan, Sugawara and Moriyoshi (1984); USA CRREL, Carpenter (1983), Janoo (1989); Utah DOT, Tuckett, et al., (1970); Technical University of Braunschweig, Germany, Arand, (1987); King, et al., (1988).

### **3.6 Three-Point Bend Specimen Test**

#### **Description**

Rice (1968a,b) and Rice and Rosengren (1968) provided the basis for this test method by identifying a line integral related to energy in the vicinity of a two-dimensional crack in the presence of plastic deformation. The line integral is termed the J-integral. Rice assumed that the deformation theory of plasticity is applicable, meaning the stresses and strains in a plastic or in an elastic-plastic body are considered to be the same as for a nonlinear elastic body with the same stress-strain curve. This further implies that the stress-strain curve is nonlinear and recoverable.

Hutchinson and Paris (1979) present a theoretical justification for use of the J-integral in the analysis of stable crack growth. Dowling and Begley

(1976) used the change in  $J$  during cyclic loading,  $\Delta J$ , to calculate fatigue crack propagation rates.

Little and Mahboub (1985) state that the critical value of the  $J$ -integral,  $J_{IC}$ , may be determined for plasticized sulfur paving mixtures following ASTM Test Method E813.  $J_{IC}$  is the energy required to drive a sharp-tipped crack or the energy released as the sharp crack tip propagates.

Under ASTM E813, three-point bend specimens are loaded monotonically at the midpoint as shown in Figure 22. A linear variable differential transformer is used to monitor the crack opening displacement. A load cell is used to monitor the applied load, and a "KRAK" gauge that is bonded to the specimen is used to monitor crack growth.

In work reported by Mahboub (1985), three-point bend specimens 1 x 2 x 8.4 in. were molded at a modified Proctor compaction effort. All specimens were notched with a chevron as specified under ASTM E399. The three-point bend specimens were loaded at the center point with an electrohydraulic closed-loop test system. The mode of testing was set at controlled displacement to produce stable crack growth during loading. The specimen was positioned on the three-point bend frame inside an environmental chamber. The temperature in the environmental chamber then was reduced to a temperature close to or below the glass transition temperature,  $T_g$ . Little and Mahboub (1985) indicate that it is not practical to use bend specimens to compute  $J_{IC}$  values at temperatures much above  $T_g$ . At temperatures above  $T_g$ , the plasticity and viscosity of the material begin to influence the response to the point that propagation of a sharp-tipped crack in the specimen is not possible because the area of the plastic zone ahead of the crack tip is too large relative to the specimen geometry. However, at temperatures close to or below  $T_g$ , the test is acceptable.

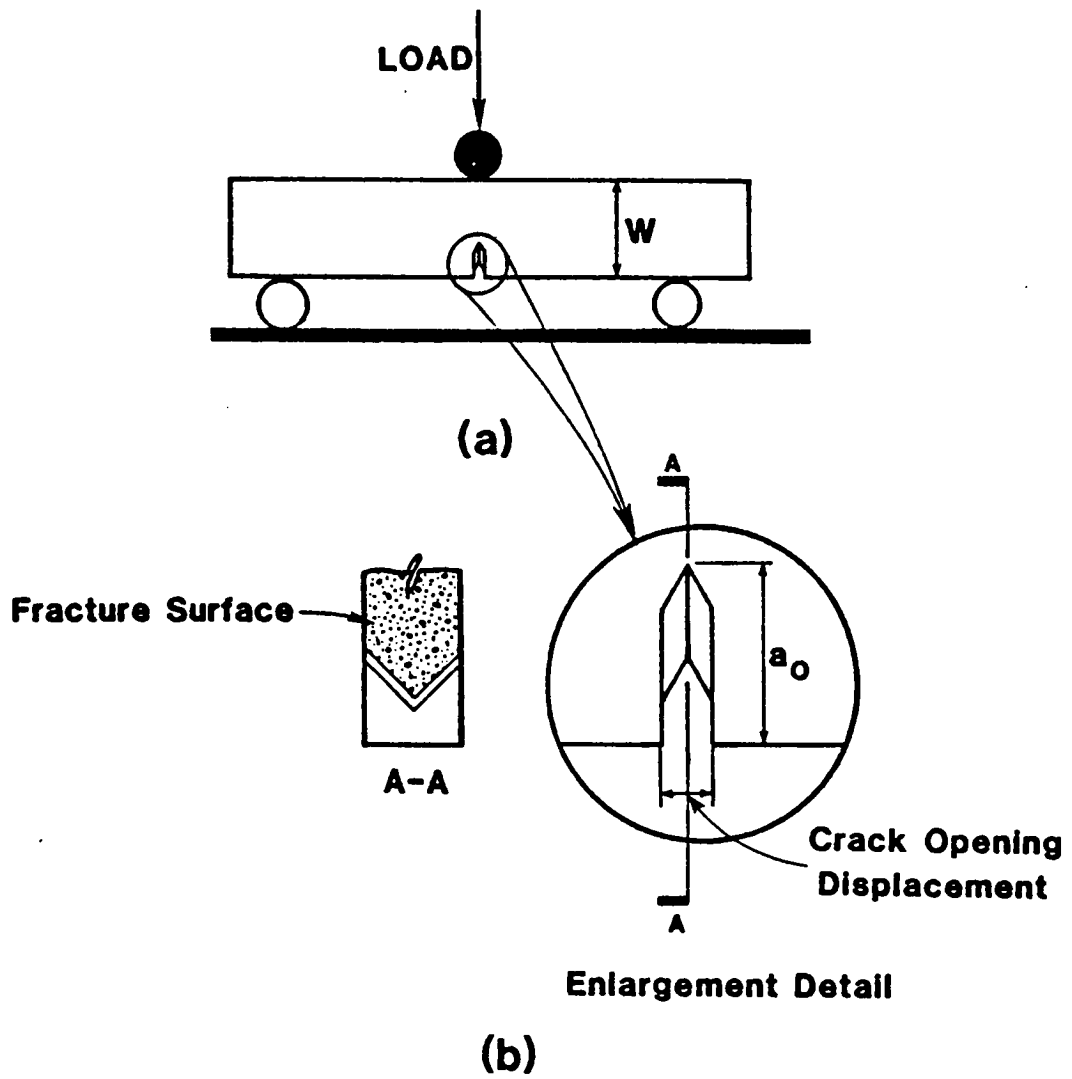


Figure 22. Three-Point Bend Specimen (after Mahboub, 1985).

After some period of time (usually about one hour), the specimen showed temperature stability, and the test was conducted. As the specimen was loaded at the center, some unloads were introduced to ensure the crack growth through the chevron was a smooth and stable process. Otherwise, a blunt chevron could store enough energy to fail the specimen instantaneously. This process was continued until the first increment of crack extension was recorded by the crack gauge, at which point an unload was introduced marking the first out of the chevron crack extension. The test was continued with unloads at different stages of crack growth until the uncracked ligament was small (about 0.20 in.). A crack opening rate of .05 in./min. and a 20-minute load ramp function were used in the experiment. Typical test results are shown in Figure 23a.

To determine  $J_{IC}$ , the load versus crack opening displacement diagram is transformed into a moment versus rotation diagram using the measured crack length at each point along the curve. The unload corresponding to the first crack growth out of the chevron was extrapolated to an X-intercept, and it was considered to be the start of the  $J_{IC}$  test. The first triangular and the subsequent trapezoidal areas under the  $M$  versus  $\theta$  curve were recorded, as shown in Figure 23b. The cumulative area at each point was regarded as the term  $A$  in the following equation

$$J = \frac{2A}{Bb} \quad (10)$$

in which,

- $B$  = specimen thickness,
- $b$  = uncracked portion of the beam.

At each stage of crack growth, the term  $J$  and the term  $\Delta a$ , defined as the difference between the length of the crack at that moment and the initial out of chevron extension, were calculated. A linear regression between  $J$  and  $\Delta a$  was established and formed the  $J_R$  line. The intercept was defined to be  $J_{IC}$ , and the slope was defined to be tearing modulus,  $T$ , as shown in Figure 24.

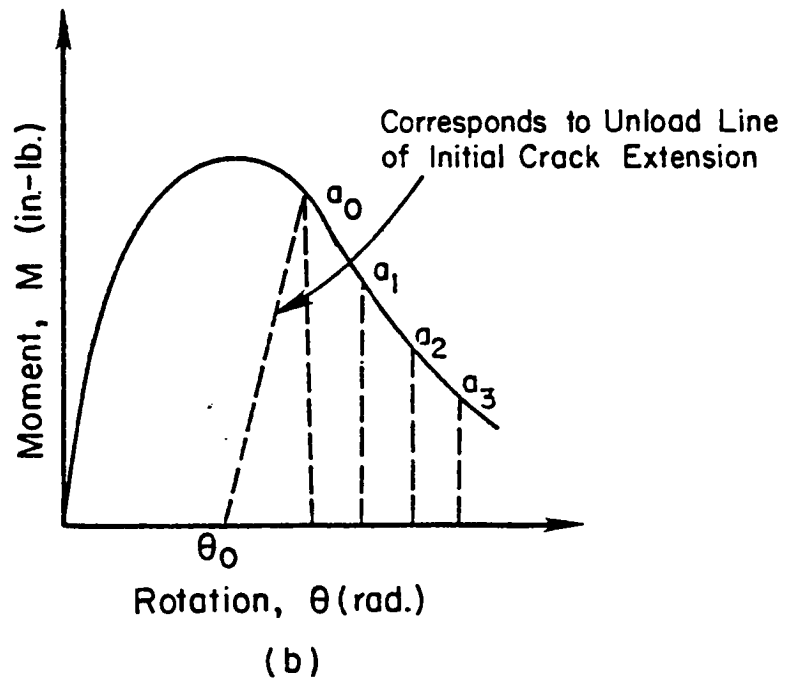
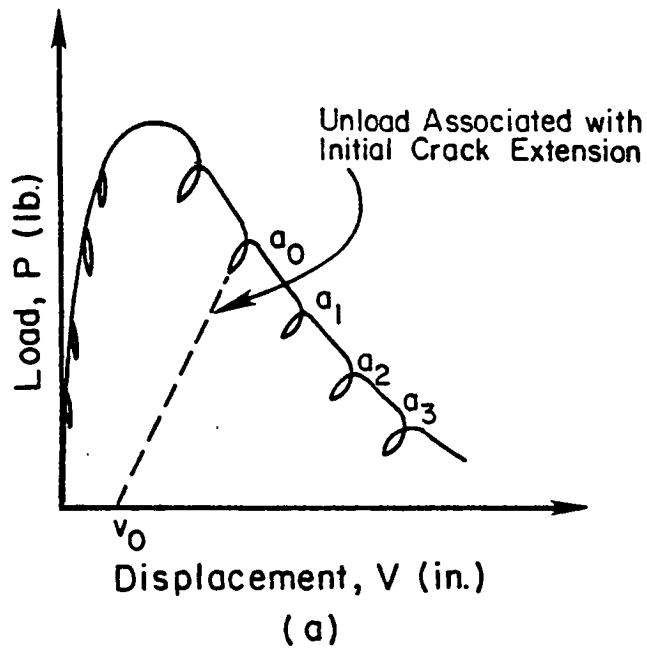


Figure 23. Three-Point Bend Specimen Load versus Displacement (a) and Its Transformation to Moment versus Rotation (b) (after Mahboub, 1985).

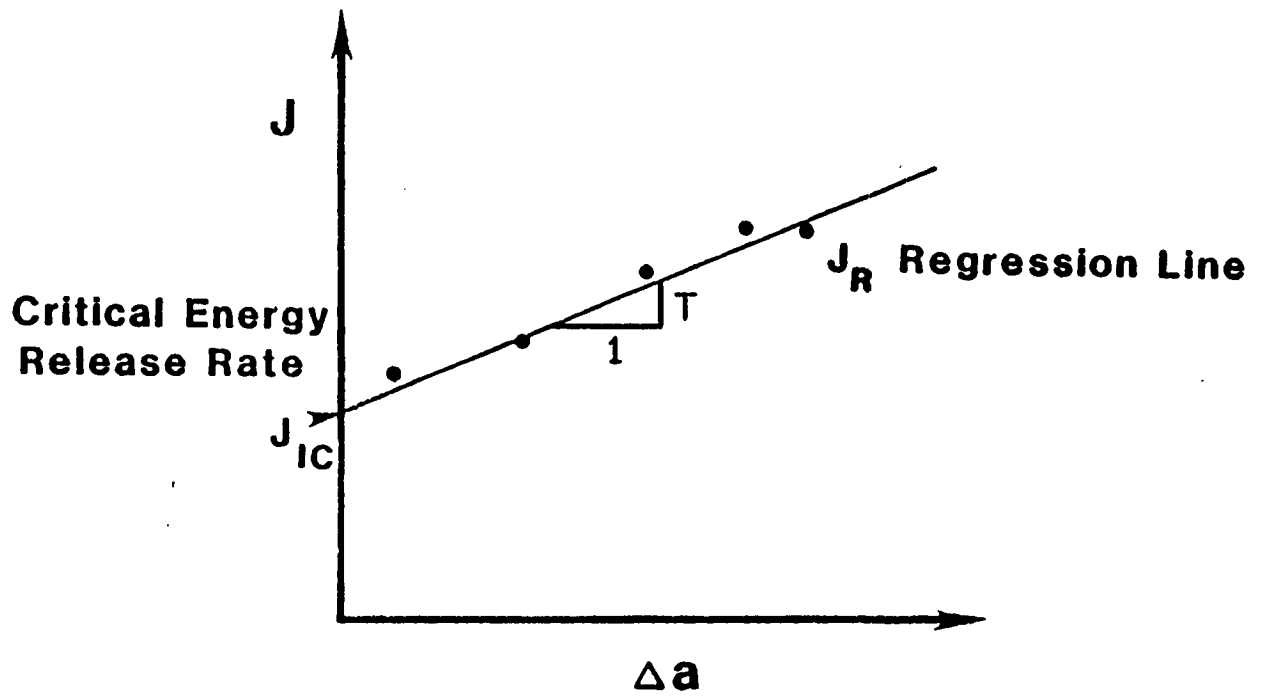


Figure 24. Illustration of Determination of Critical Energy Release Rate,  $J_{IC}$ , and Tearing Modulus,  $T$  (after Mahboub, 1985).



The traditional J-integral testing procedure requires at least four samples with different notch lengths. Each sample is loaded monotonically until failure. Fortunately, another technique has been developed that enables  $J_{IC}$  to be determined from multiple unloads of a single specimen (Landes and Begley, 1976).

### **Test Condition Parameters**

Temperature, specimen geometry and volume, crack opening rate, load ramp function.

### **Properties Measured**

Critical energy release rate,  $J_{IC}$ , and tearing modulus,  $T$ .

### **Agency/Institutional References**

Texas A&M University Mahboub (1985), Little and Mahboub (1985).

## **3.7 C\*-Line Integral Test**

### **Description**

The method of determining the  $C^*$  parameter experimentally was suggested by Landes and Begley (1976b) and is shown schematically in Figure 25. In this method, as reported by Abdulshafi and Kaloush (1988), multiple specimens are subjected to different constant displacement rates. The load ( $P$ ) per unit crack plane thickness and the crack length ( $a$ ) are measured as a function of time, as shown in Step 1. This step represents the actual data collected during the test. Because the tests are conducted at a constant displacement rate, time and displacement are the independent variables. Load and crack length are dependent variables. The data in Step 1 are cross-plotted to yield the load as a function of the displacement rate ( $\dot{\Delta}$ ) (from tests at several displacement rates) for fixed crack lengths, as shown in Step 2. The area

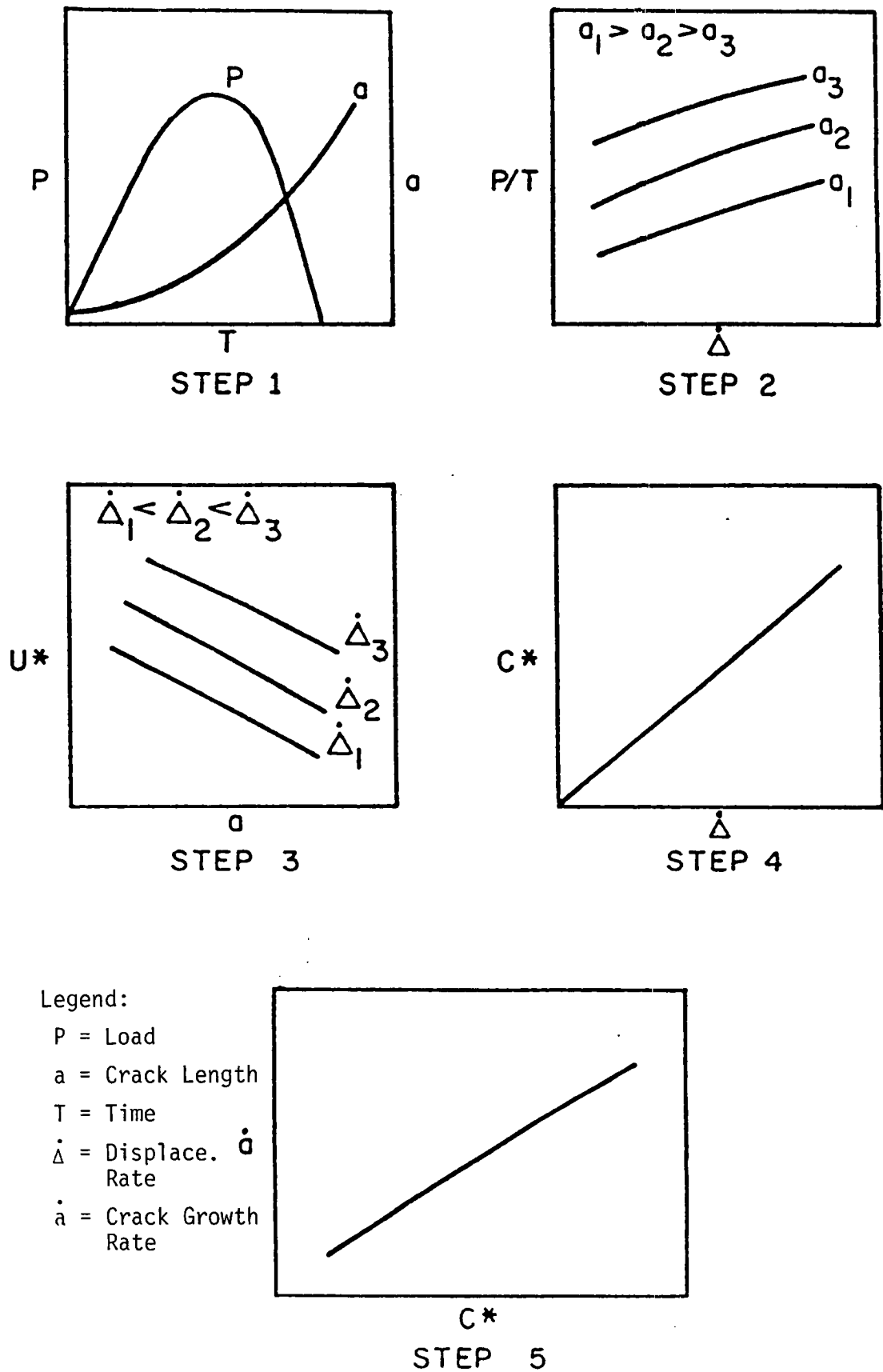


Figure 25. Steps in Determination of  $C^*$  Line Integral (after Abdulshafi 1983b).

under the curve in Step 2 is the rate of work done,  $U^*$  per unit of crack plane thickness. This is shown plotted against the crack length, as in Step 3. The energy rate interpretation of  $C^*$  is given as the power difference between two identically loaded bodies having incrementally differing crack lengths by:

$$C^* = \frac{1}{b} \left. \frac{dU^*}{da} \right|_{\dot{\Delta}} \quad (11)$$

in which,

- $b$  = thickness of specimen in crack plane
- $U^*$  = power of energy rate for a load  $P$  and displacement rate,  $\dot{\Delta}$
- $a$  = crack length

Consequently, the slope of the curve in Step 3 is  $C^*$ . Finally,  $C^*$  is plotted as a function of the crack growth rate, as shown in Step 4, or the crack speed is plotted as a function of  $C^*$ , as shown in Step 5. This method of  $C^*$  determination is called the multiple-specimen method.

Abdulshafi (1983b) adopted this method to evaluate the critical release rate line integral of asphalt concrete mixtures. He used the test configuration shown in Figure 26. The dimensions of the diametral specimen, 4-in. diameter and a 2.5-in. thickness, are compatible with the requirement of a plane strain loading condition. (A minimum thickness of 2 in. is recommended.) A right-angled wedge is cut into the disc specimen to accommodate the loading device. The wedge should be cut to a depth of 0.75 in. along the specimen diameter and should extend over the entire thickness. Care should be exercised to ensure symmetry of the wedge about the vertical axis and smoothness of cut surfaces for proper contact with the loading steel wedges. A small, artificial crack is sawed at the tip of the wedge (notch) to channelize crack initiation. It is preferable that a light-colored vertical strip that includes the notch tip be painted on the specimen to clearly distinguish crack

$$C^* = \frac{1}{b} \left. \frac{du^*}{dc} \right|_{\dot{\Delta}}$$

b = Sample Thickness

u\* = Power of Energy Rate  
for a Load p and  
Displacement Rate

a = Crack Length

| $\dot{\Delta}$  : Means with Displacement  
Rate Held Constant

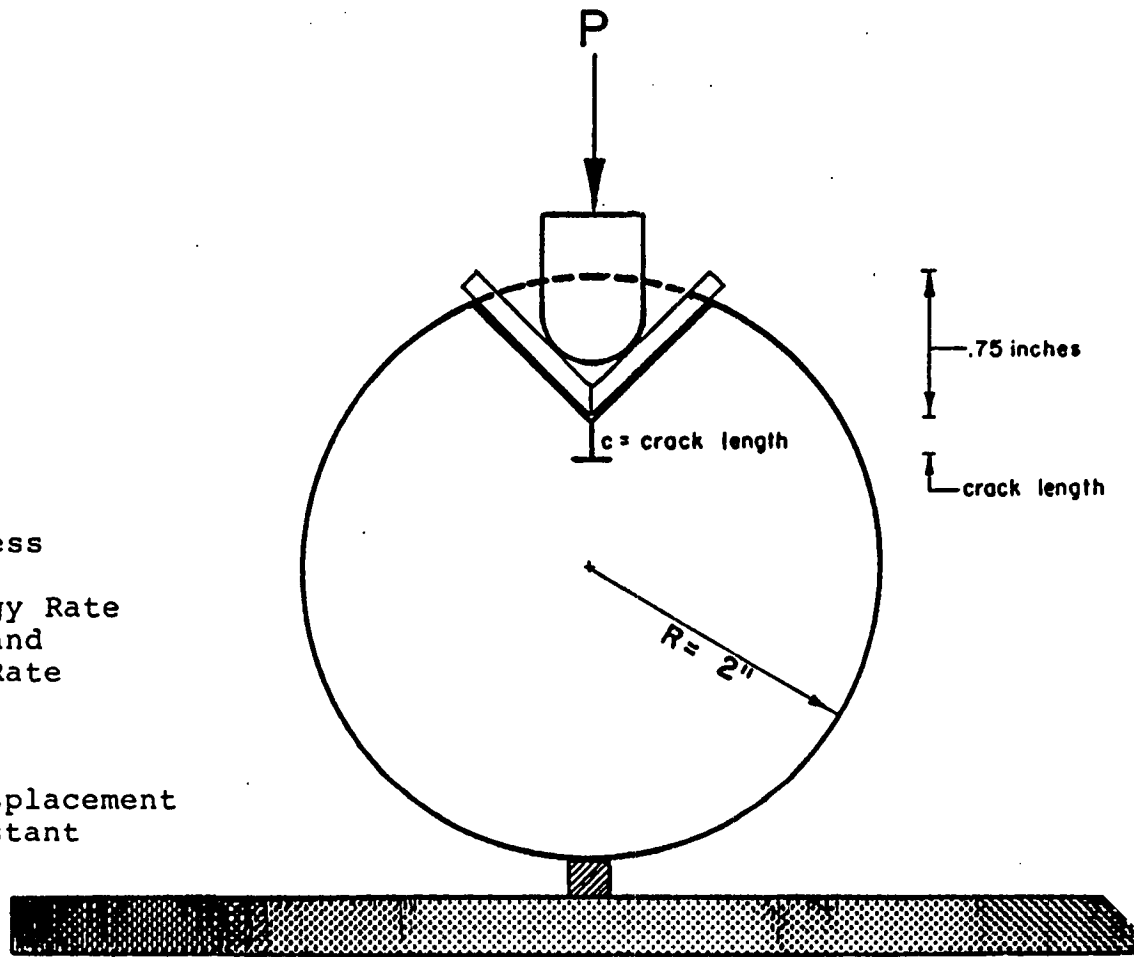


Figure 26. Typical C\*- Test Configuration (after Abdulshafi, 1983b).

initiation and propagation processes. A vertical line extending from the notch tip to the contact point of the load seat strip should be marked and scaled. A gradually and slowly increasing monotonic load is applied to the sample until a crack is noticed. The load is maintained until the required crack size is reached. A minimum of three displacement rates is required to evaluate the  $C^*$ -line integral. Duplicate specimens are recommended.

### **Test Condition Parameters**

Temperature, displacement rate, specimen size.

### **Properties Measured**

Energy release rate line integral,  $C^*$ .

### **Agency/Institution Reference**

CTL International, Inc., Abdulshafi and Kalosh (1988); The Ohio State University, Abdulshafi (1983b), Abdulshafi and Majidzadeh (1985).

## **3.8 Coefficient of Thermal Expansion and Contraction Test**

### **Description**

The test frame used by Jones, et al., (1968) to determine thermal coefficients of contraction for asphalt mixes is shown in Figure 27. The test frame is placed on a table in a walk-in freezer. A smaller environmental chamber is placed around the test frame. The environmental chamber has slits in each end to allow deflection gauges to come into contact with metal pins at the ends of the specimen. The environmental chamber has heating coils so that the temperature can be cycled. Two different restraint conditions are considered, namely, (1) free movement condition, and (2) friction base condition. The free movement condition is obtained by placing the specimen on a base that provides nearly frictionless movement (small ball bearings were placed on a

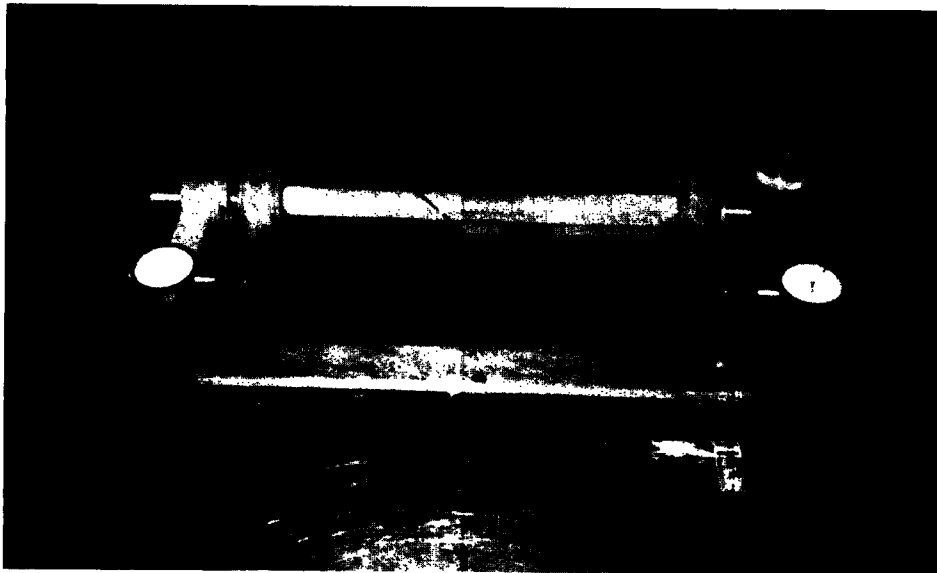
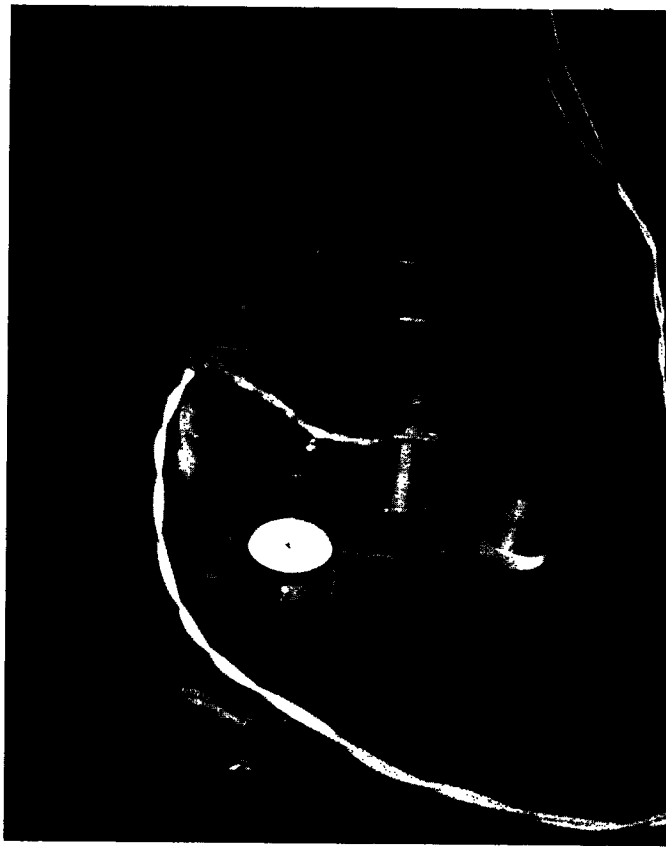


Figure 27. Utah DOT Coefficient of Thermal Contraction Test Frame.

pane of glass). The friction base condition was obtained by gluing grit No.40-D sandpaper to a plywood board. The environmental chamber does not cover the main bar of the test frame. The test is initiated by setting the cold room temperature to  $-10^{\circ}\text{F}$ . The  $3 \times 3 \times 16$  in. specimen is subjected to a uniform temperature change of  $12^{\circ}\text{F/hr}$  (i.e.,  $5 \text{ min}/^{\circ}\text{F}$ ). The specimen temperature is raised to  $80^{\circ}\text{F}$  and then allowed to cool back to  $-10^{\circ}\text{F}$ .

Osterkamp, et al., (1986) used an LVDT and a precision push-rod-type dilatometer mounted on a tripod with fused quartz glass legs to determine thermal contraction coefficients of asphalt mixes. A metal base plate was used to support the tripod and specimen, which was placed in a cylinder between the legs of the tripod. The apparatus was placed in a well-stirred low temperature bath. Specimen temperatures were measured by a thermistor placed at the mid-point of the specimen. The experimental procedure involved placing the specimen in the apparatus and allowing it to equilibrate to an initial temperature of approximately  $10^{\circ}\text{C}$ . The bath then was lowered at a rate of about  $7^{\circ}\text{C/hr}$  to the final temperature (approximately  $-55^{\circ}\text{C}$ ). The specimen was allowed to equilibrate at this temperature, and then the bath was heated at a rate of about  $5^{\circ}\text{C/hr}$  to the initial temperature and the specimen again was allowed to equilibrate. The specimen was subjected to 3 to 6 thermal cycles. The specimen dimensions were not given, but it was noted that the specimens were rectangular bars cut from field core samples.

### **Test Condition Parameters**

Specimen geometry and volume, number of thermal cycles, and rate of cooling.

### **Properties Measured**

Thermal expansion and contraction coefficients.

## Agency/Institutional References

Utah DOT, Jones, et al., (1968); Alaska DOT, Osterkamp, et al., (1986).

### 3.9 Determination of Thermal Conductivity and Specific Heat Capacity

The thermal conductivity,  $K$ , and specific heat capacity,  $C$ , of an asphalt concrete mix are required to compute the thermal regime in the asphalt concrete layer. The thermal conductivity expresses the rate of heat flow through a unit area under a unit temperature gradient. Commonly used units for  $K$  are  $(\text{BTU/hr})/(\text{ft}^2)/(^{\circ}\text{F/ft})$  or  $(\text{Cal/sec})/(\text{cm}^2)/(^{\circ}\text{C/cm})$ . The specific heat capacity is the thermal energy required to cause a 1-degree change in a unit mass of material. Commonly used units are  $(\text{BTU/lbs})/(^{\circ}\text{F})$  or  $(\text{Cal/gm})/(^{\circ}\text{C})$ . The thermal conductivity and specific heat capacity of a mix are governed by the thermal properties of the aggregate and bituminous binder. Thermal conductivity and specific heat capacity values of asphalt concrete mixes may be measured in the laboratory. However, it has been determined by a number of researchers that these properties do not vary significantly between mixes. Consequently, values for thermal conductivity and specific heat capacity are often assumed to be within the following ranges:

$$K = 0.82 - 0.86 (\text{BTU/hr})/(\text{ft}^2)/(^{\circ}\text{F/ft})$$

$$C = 0.20 - 0.22 (\text{BTU/lbs})/(^{\circ}\text{F})$$

The thermal diffusivity,  $\alpha$ , is an index of the facility with which a material will undergo temperature change. It is defined by the ratio

$$\alpha = \frac{K}{C} \tag{12}$$

The thermal diffusivity for asphalt concrete mixes is not measured, but is calculated with a knowledge at the thermal conductivity and specific heat capacity.



## 4.0 RELATIONSHIP BETWEEN TEST PROCEDURES and FIELD PERFORMANCE

### 4.1 Description of Mechanistic Models

A number of analytical models have been proposed to relate the properties measured in the test methods discussed in Section 3.0 to field performance.

Four thermal cracking models have been considered and reviewed, as follows:

- COLD MODEL (Finn, et al., 1986) – The model was developed based on principles given by Hills and Brien (1966) (re. equation (1)). The model is based on the hypothesis that low temperature cracking occurs only when the thermally induced tensile stress in the pavement exceeds the tensile strength (re. Figure 3). This failure condition generally is associated with a limiting temperature (i.e. the fracture temperature), which in turn primarily is dependent upon the asphalt cement properties. The flow diagram for the model is given in Figure 28. The COLD program calculates the temperature distribution within the asphalt layer and its variation from day to day. The following information is required for program COLD:

Section thickness

Thermal properties of component layers

Ambient temperatures and solar radiation

Initial ambient temperature gradient

Creep modulus (stiffness) of asphalt concrete versus temperature for the mix

Tensile strength of asphalt concrete at slow rates of loading (.01 in./min.) versus temperature of asphalt concrete.

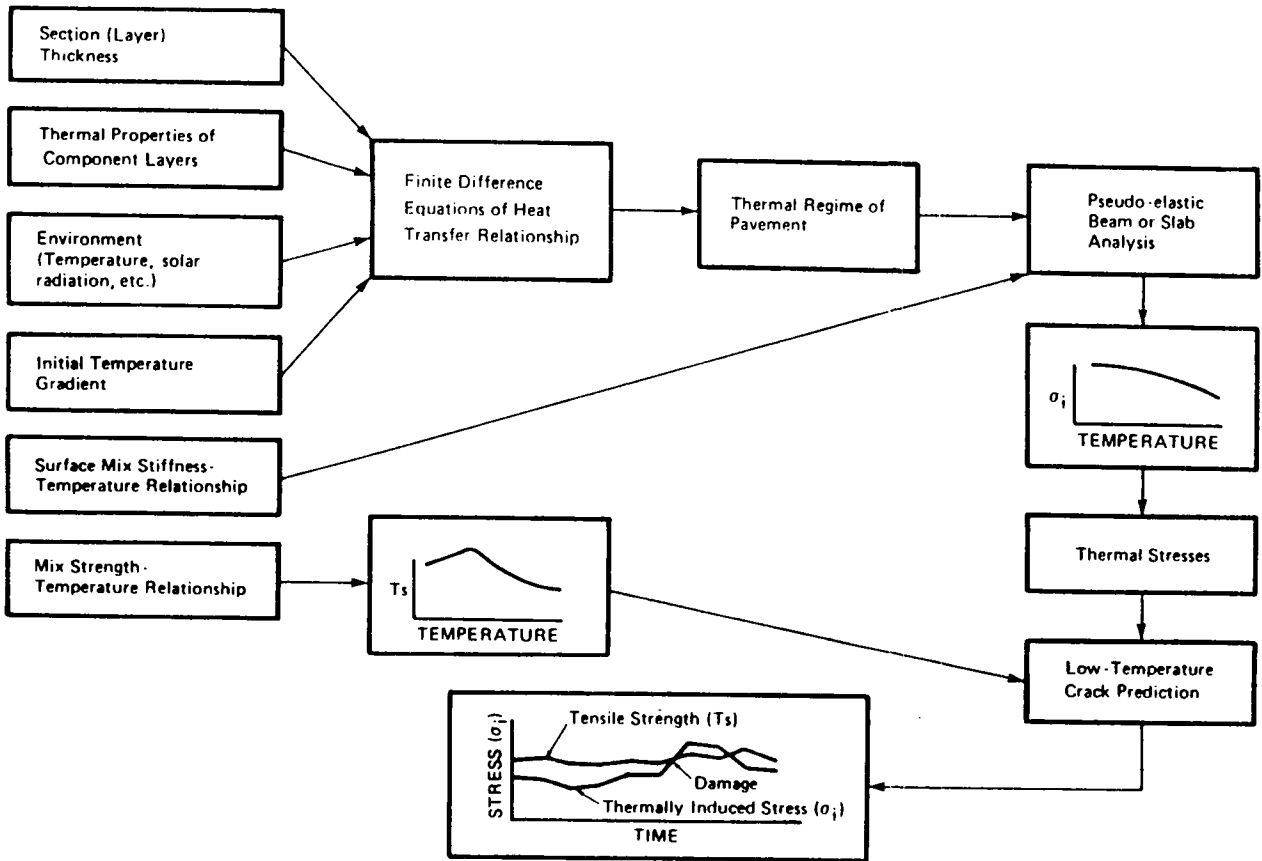


Figure 28. Flow Diagram for Program COLD (after Finn, et al., 1986).

Appendix C of NCHRP 291 (Finn, et al., 1986) provides a good description of the model program. The results from direct or indirect tension tests are used in the model.

- UNIVERSITY OF FLORIDA MODEL (Ruth, et al., 1982) – The results from indirect tensile tests, low temperature viscosity tests from the Schwyer Rheometer, and indirect creep tests are used to develop an equation to predict creep deformation. Cracking will occur when the thermally induced strain exceeds the ability of the sample to relax the creep strain developed under the effect of a thermal stress on the sample. They derive an equation to predict the incremental thermal stresses in the pavement structure. The model uses more fundamental asphalt properties than any other model that predicts low temperature cracking. The model makes a correction for the creep of the mixture under the thermal stress. A summary of the model is given by Carpenter (1983) and Anderson, et al., (1989).
- TEXAS A&M UNIVERSITY MODEL (Lytton, et al., 1983) – This is a fracture-mechanics approach to study thermal fatigue cracking. The model is supported by the computer program THERM. Thermal fatigue is defined as fatigue caused by thermal cycling below 75°F (25°C). The model requires daily temperature data and climatic factors, such as solar radiation, air temperature and wind speed, to calculate the temperature distribution in the surface layer from the modified Barber equation. The stiffness temperature relationship of the asphalt concrete is obtained using a computerized version of the van der Poel nomogram from the standard asphalt cement and mixture characterization values. The model provides an option for aging the asphalt concrete. Under one option, the entire thickness of asphalt

concrete is aged, while under the second option, only the upper .5 - 1 in. of surface layer is aged.

In the model, the thermal stresses are not compared directly with the tensile strengths to identify the onset of a thermal crack. The principles of viscoelastic fracture mechanics are used to accumulate damage under repeated temperature cycles. Miner's hypothesis is used to accumulate the damage produced by any one cycle. The coefficient of thermal contraction cannot be specified in this model. This is a significant shortcoming because the coefficient of thermal contraction is an important parameter.

- UNIVERSITY OF TEXAS MODEL (Shahin and McCullough, 1972) - This model, supported by the computer program TC-1, is the first practical representation of low temperature cracking combined with thermal fatigue cracking. It also incorporates a treatment of the statistical variability of materials. The temperatures in the pavement structure are calculated with the modified Barber equation using average temperature and climate data for the location being analyzed. The input data can include air temperature, wind velocity, solar radiation, asphalt concrete thermal properties and depth below the pavement surface. The stiffness relationships in the model are obtained by indirect estimation (i.e., using the van der Poel (1954) nomogram and later modified by Heukelom and Klomp (1964)). The procedure to calculate thermal stresses involves the testing of an actual sample in the thermal-stress situation using only the average parameters that might be expected in the field. Probabilistic methods are used to predict whether the thermal stresses exceed the mixture strength and, therefore, the probability of occurrence of low temperature cracking. The thermal fatigue module in the model

uses the standard load-fatigue relationship and Miner's hypothesis to accumulate the damage associated with one thermal cycle. The program incorporates aging equations in an attempt to predict the aging characteristics of the asphalt cement. Carpenter (1983) and Anderson, et al., (1989) provide a good summary of the model.

#### **4.2 Input and Output Data for Mechanistic Models**

A summary of input and output data for thermal cracking models given by Anderson, et al., (1989) is reproduced in Table 1. It is of interest to note that the thermal stress versus temperature relationship is not input directly in any model.

Table 1. Summary of Input and Output Data for Low-Temperature Cracking Models (modified after Anderson, et al., 1989)

Properties	TC-1	COLD	THERM	Ruth
<u>INPUTS:</u>				
Stiffness of Original Asphalt vs. Temperature (Loading Time = 20,000 s using McLeod's version of Van der Poel's nomograph)				
Asphalt Stiffness vs. Temperature, Van der Poel's nomograph as modified by Heukelom and Klomp				
Loading Time = 20,000 s	X			
Loading Time = 7,200 s	X	X		
Static Compression Modulus of Mixture vs. Mix Viscosity				X
Asphalt Specific Gravity	X			X
Original Penetration at 77°F (25°C)	X	X	X	
Original Penetration at 41°F (5°C)				
Original Softening Point of the Asphalt, °F	X		X	
Thin Film Oven Test, Weight Loss and Retained Penetration	X			
Volumetric Concentration of the Aggregate	X		X	
Penetration Index: Penetration at 77°F (25°C) and Kinematic Viscosity at 275°F (135°C)	X		X	
Absolute Viscosity vs. Temperature (Schweyer rheometer)				X
Indirect Tensile Strength vs. Temperature (0.01 in./min) (0.25 mm/min)	X	X		
Linear Thermal Coefficient of Expansion/Contraction		X		X
Thermal Coefficient of Expansion/Contraction vs. Temperature	X			
Thermal Fatigue Constants	X			
Surface Absorptivity	X	X	X	
Mix Conductivity	X	X	X	
Mix Specific Heat	X	X	X	
Mix Density	X	X	X	

Table 1. Summary of Input and Output Data for Low-Temperature Cracking Models (modified after Anderson, et al., 1989)

Properties	TC-1	COLD	THERM	Ruth
Emissivity		X		
Connection Coefficient		X		
Age	X		X	
Thickness	X	X	X	X
Winter Design Temperature				
Moisture Content		X		
Wind Velocity	X		X	
Average Temperature	X		X	
Yearly Temperature Range	X		X	
Daily Temperature Range (Cooling Rate)	X		X	X
Solar Radiation	X	X	X	
Subgrade Type				
<b>OUTPUTS:</b>				
Cracking Index with Time			X	
Area Cracking with Time	X			
Critical Temperature at which Cracking Occurs		X		X

## 5.0 EVALUATION OF TEST METHODS AND PROPOSED TEST PROGRAM

### 5.1 Evaluation of Test Methods

Eight test systems/methods were identified in Section 3.0. These methods were evaluated in terms of the following criteria:

- 1) Simulation of field conditions
- 2) Application of test results to mechanistic models
- 3) Suitability for aging and moisture conditioning
- 4) Potential to accommodate large stone mixes
- 5) Ease of conduct
- 6) Cost of equipment

A summary of the evaluation is given in Table 2. The criteria listed above are given in their relative order of importance with respect to meeting the overall objectives of the project. The most important criterion is to identify a test that relates as closely as possible to the field conditions that are being considered.

Only two of the test methods actually simulate the field conditions, namely, the thermal stress restrained specimen test and the coefficient of expansion and contraction test. The remaining methods provide (1) low-temperature stress-strain characteristics of an asphalt concrete specimen and, when the specimen fails during loading, the tensile strength, or (2) an energy release rate fracture mechanics parameter, but these properties are only indirect measures of the response of the mix to cooling.

The results obtained from the load-deformation tests indirectly are applicable for use in mechanistic models. The designator "indirectly applicable" is given because the results from these tests often support the determi-



Table 2. Evaluation of Thermal Cracking Test Methodologies.

Test Method	Agency/ Institutional Reference	Properties Measured	Simulation of Field Conditions	Application of Test Results to Mechanistic Models	Suitability for Aging and Moisture Conditioning	Potential to Accommodate Large Stone Mixes	Ease of Conduct	Cost/ Availability of Equipment	Comments
(1) Indirect Diametral Tension	Univ. of Florida Univ. of Alberta	Low temp. tensile stress/strain char.; tensile strength	No	Indirectly applicable to low temp. cracking models	Moderate	High	Easy	Mod. cost; generally available	Well-docum. pro- cedure; significant prior use in pro- fession
(2) Direct Tension - Constant Rate of Extension	Univ. of Water- loo; Asphalt Inst.; Tech. Univ. of Braunschweig	Tensile stress/ strain char.; tensile strength	No	Indirectly applicable to low temp. cracking models	Moderate	High	Easy	Mod. cost; generally available	Well-docum. pro- cedure; significant prior use in pro- fession
(3) Tensile Creep	Univ. of Water- loo; Ontario DOT	Tensile stress/ strain char.; tensile strength	No	Indirectly applicable to low temp. cracking models	Moderate	High	Easy	Mod. cost; generally available	No longer used in profession
(4) Flexural Bending	Univ. of Wisconsin Inst.	Stress/strain char.; tensile strength	No	Indirectly applicable to low temp. cracking models	Low	High	Easy	Mod. cost; generally available	No longer used in profession
(5) Thermal Stress Restrained Specimen	UC Berkeley; British Petro.; Hokkaido Univ.; USACREL; Utah DOT; Tech. Univ. of Braunschweig	Low temp. thermal stress char.; tensile strength; fracture temp.	Yes	Directly applicable to low temp. cracking & fatigue models	Moderate	High	Easy	Mod. cost; not gener- ally avail- able	Well-docum. pro- cedure; significant prior use in pro- fession
(6) Three Point Bend Specimen Test	Texas A&M Univ.	Critical energy release rate	No	Indirectly applicable	Low	Low	Difficult	Mod. cost; generally available	Well-docum. pro- cedure but may not be applicable to mixes with coarse aggregate
(7) C*-Line Integral Test	CTL Labs.; The Ohio State Univ.	Energy release rate line inte- gral	No	Indirectly applicable	Moderate	Moderate	Moderate	Mod. cost; generally available	Well-docum. pro- cedure
(8) Coefficient of Thermal Expan- sion & Contrac- tion	Utah DOT; Alaska DOT;	Thermal expansion & contraction coefficient	Yes	Indirectly applicable; used in conj. w/tensile stress/strain char.	Moderate	High	Easy	Low cost; not gener- ally avail- able	Well-docum. procedure

nation of the thermal stress/temperature relationship (re. Figure 4 and equation (1)), but they are not a direct measure of this relationship. The coefficient of thermal contraction also is indirectly applicable since it is multiplied by the temperature change and stiffness modulus to arrive at the thermal stress relationship (re. equation (1)). In many of the models, the coefficient of thermal contraction is assumed. The results from the fracture mechanics tests (i.e. three-point bend and C\*-line integral) also are indirectly applicable to a mechanistic model as fracture is induced by an applied load and not with a temperature drop or cycling.

The only results directly applicable to the existing mechanistic models are the thermal stress versus temperature relationship obtained in a thermal stress restrained specimen test. However, the models that presently are available do not allow this relationship to be input, as the algorithms developed to support the models calculate the relationship from indirect measurements of thermal response or properties of the asphalt cement. Further, the results from thermal cycling experiments conducted with the thermal stress restrained specimen test system will support future thermal fatigue models.

The assessment of the suitability of the test method for aging and moisture conditioning is speculative. Those test methods that could employ cylindrical specimens are believed to be moderately suitable for aging and moisture conditioning; the flexural bending test uses a rectangular beam specimen, which has low suitability for aging and moisture conditioning.

For all practical purposes, the tensile creep test and flexural bending tests presently are not used by practitioners/researchers to determine low temperature tensile stress/strain and strength characteristics of asphalt concrete mixes.

A consideration of the potential to accommodate large stone mixes (maximum aggregate particle size greater than 1 in.) arises from the current

trend to use these to reduce rutting. All of the test methods identified can accommodate large stone mixes or could be easily modified to accommodate large stone mixes, except the fracture mechanics test methods. The three-point bend specimen test presently is limited to specimens with a fine aggregate and the C\*-line integral test is limited to a maximum aggregate size of 3/4 in.

All of the test methods are relatively easy to conduct, except the three-point bend specimen and C\*-line integral. These are identified as difficult and moderate, respectively, owing to the requirement to notch the specimen and monitor the rate of crack propagation during the conduct of the test. The test procedures for the load deformation tests (i.e., indirect diametral and direct tension, tensile creep, and flexural bending) are well-established and documented. With respect to indirect diametral and direct tension, the test equipment associated with the test methods is in routine use in many laboratories. The test equipment for tensile creep, flexural bending, thermal stress, and coefficient of expansion/contraction is not routinely used by many laboratories. The test procedures for the three-point bend specimen tests are documented, but are in the first generation of use.

The cost of the test equipment is moderate, that is, from \$10,000 to \$30,000 (1989 cost estimate). The cost of the coefficient of thermal expansion/contraction equipment is low, that is, under \$10,000 (1989 cost estimate). These cost estimates reflect a temperature-control bath or chamber as a part of the test system.

## **5.2 Proposed Test Program**

Based on the evaluation of the test systems/methods presented in section 5.1, it would appear that four test systems/methods warrant further consideration in a laboratory test program, as follows:

- 1) Direct Tension–Constant Rate of Extension test
- 2) Thermal Stress Restrained Specimen test
- 3) C\*–Line Integral test
- 4) Coefficient of Thermal Expansion and Contraction test

The proposed test programs for the several preliminary evaluations are listed in Table 3. The details of the experimental treatments are given in Tables 4–8. All tests associated with the fractional or full factorial designs noted will be replicated to provide the desired precision in the test results.

The indirect diametral tension, thermal stress restrained specimen, and coefficient of thermal expansion/contraction tests will be conducted at Oregon State University. Thermal stress restrained specimen and coefficient of thermal expansion/contraction tests also will be conducted at USA CRREL. Direct tension–constant rate of extension tests will be conducted at the University of Waterloo. This program will be expanded to include other asphalts and aggregates and moisture and aging conditioning at a later date.

Table 3. Proposed Test Programs for the Preliminary Evaluation of Test Systems/Methods.

Type of System	Table	Design	Fraction	Number of Main Effects and Two-Factor Interactions
Direct Tension Constant Rate of Expansion	4	$2^{5-1} \cdot 3^1$	1/2	27
Thermal Stress Retained Specimen	5	$2^{6-1}$	1/2	21
Thermal Fatigue Retained Specimen	6	$2^5$	Full	15
C*-Line Integral	7	$2^{5-1} \cdot 3^1$	1/2	27
Coefficient of Thermal Expansion and Contraction	8	$2^4$	Full	10

Table 4. Test and Material Variables for Load-Deformation Tests.

Variable	Type	Number to be Considered
Deformation rate	Test	2
Temperature	Test	3
Aggregates	Material	2
Air void content	Material	2
Asphalt cement	Material	4
Asphalt content	Material	1
Aging	Material	1
Moisture conditioning	Material	1

Table 5. Test and Material Variables for Thermal Stress Restrained Specimen Tests.

Variable	Type	Number to be Considered
Cooling rate (5°C/hr and 20°C/hr)	Test	2
Cooling rate w/relaxation (@ -15°C and -25°C)	Test	2
Aggregate	Material	2
Air void content	Material	2
Asphalt cement	Material	4
Asphalt content	Material	1
Aging	Material	1
Moisture conditioning	Material	1

Table 6. Test and Material Variables for Thermal Cycle Restrained Specimen Tests.

Variable	Type	Number to be Considered
Thermal cycle level	Test	2
Aggregates	Material	2
Air void content	Material	2
Asphalt cement	Material	4
Asphalt content	Material	1
Aging	Material	1
Moisture conditioning	Material	1

Table 7. Test and Material Variables for C\*-Line Integral Tests.

Variable	Type	Number to be Considered
Displacement rate	Test	3
Temperature	Test	2
Aggregates	Material	2
Air void content	Material	2
Asphalt cement	Material	4
Asphalt content	Material	1
Aging	Material	1
Moisture conditioning	Material	1

Table 8. Test and Material Variables for Coefficient of Thermal Expansion/Contraction Test.

Variable	Type	Number to be Considered
Cooling rate	Test	1
Aggregates	Material	2
Air void content	Material	2
Asphalt cement	Material	4
Asphalt content	Material	1
Aging	Material	1
Moisture conditioning	Material	1

## 6.0 CONCLUSIONS AND RECOMMENDATIONS

### 6.1 Preliminary Conclusions

- Previous research to evaluate asphalt concrete mix properties relative to predicting low temperature and thermal fatigue cracking has included tests to characterize the thermal properties (coefficient of thermal contraction, thermal conductivity and specific heat capacity), temperature-stress-strain-strength-fatigue-time relationship, and thermal stress-temperature relationship.
- It may not be possible to derive all needed input parameters to an existing analytical model with the test results obtained from a single specimen. Further, it may not be possible to use the same specimen geometry in a test to evaluate thermal properties compared to a test to evaluate stress-strain-strength-time-fatigue properties.
- Several low temperature cracking models are available that would allow a sensitivity analysis to be conducted to eliminate the requirement to measure one or more of the input parameters in the lab. This sensitivity analysis should be coupled with the known range of many of the parameters that are required for the models.

### 6.2 Recommendations

- The test program identified under section 5.2 should be conducted to provide a preliminary evaluation of the suitability of selected test systems/methods (1) for standardization, and (2) to provide input parameters to mechanistic models for low temperature and thermal fatigue cracking.



## REFERENCES

- Abdulshafi, A. (1983a). "Viscoelastic/plastic characterization, rutting and fatigue of flexible pavements." Ph.D. thesis submitted to The Ohio State University.
- Abdulshafi, O. (1983b). "Rational material characterization of asphalt concrete pavements." Ph.D. thesis submitted to The Ohio State University.
- Abdulshafi, A. and K. Majidzadeh. (1985). "J-integral and cyclic plasticity approach to fatigue and fracture of asphaltic mixtures." *Transportation Research Record*, No. 1034, 112-123.
- Abdulshafi, A. and K.E. Kaloush. (1988). "Modifiers for asphalt concrete." ESL-TR-88-29, Air Force Engineering and Services Center, Tyndall Air Force Base, FL.
- Ad Hoc committee of The Asphalt Institute. (1981). "Design techniques to minimize low temperature asphalt pavement transverse cracking." *RR-73-1*.
- Anderson, D.A., D.W. Christenson, R. Dongre, M.G. Sharma, J. Runt, and P. Jordhal. (1989). "Asphalt behavior at low service temperatures." *Report No. FHWA-RD-88-078*, The Pennsylvania Transportation Institute, University Park, PA.
- Anderson, K.O., and S.C. Leung. (1987). "Applications of a method for evaluation of low temperature tensile properties of asphalt concrete." *Proc., Paving in Cold Areas Mini-Workshop*, 335-366.
- Arand, W. (1987). "Influence of bitumen hardness on the fatigue behavior of asphalt pavements of different thickness due to bearing capacity of subbase, traffic loading, and temperature." *Proc., 6th International Conference on Structural Behavior of Asphalt Pavements*, University of Michigan, 65-71.
- Benson, P.E. (1976). "Low temperature transverse cracking of asphalt concrete pavements in Central and West Texas." *TTI-2-9-72-175-2F*, Texas Trans. Inst., Texas A&M University.
- Bloy, L.A.K. (1980). "Asphalt rheology for prediction of low-temperature behavior of asphalt concrete pavements." MS. Thesis, University of Florida.
- Burgess, R., O. Kopvillem, and F. Young. (1971). "Ste. Anne Test Road: relationship between predicted fracture temperatures and low-temperature field performance." *Proc., AAPT*, Vol. 40, 148-193.
- Busby, E.O., and L.F. Rader. (1972). "Flexural stiffness properties of asphalt concrete at low temperatures." *Proc., AAPT*, Vol. 41, 163-187.
- Carpenter, S.H. (1983). "Thermal cracking in asphalt pavements: an examination of models and input parameters." USA CRREL.
- Carpenter, S.H., and T. VanDam (1985). "Evaluation of low temperature performance of asphalt cements." USA CRREL.

Christison, J.T., and K. Anderson. (1972). "The response of asphalt pavements to low-temperature climatic environments." *Proc., Third International Conference on the Structural Design of Pavements*, London.

Christison, J.T., D.W. Murray, and K.O. Anderson. (1972). "Stress prediction and low-temperature fracture susceptibility of asphaltic concrete pavements." *Proc., AAPT*, Vol. 41, 494-523.

Committee on Characteristics of Bituminous Materials. (1988). "Low temperature properties of paving asphalt cements." *State-of-the-Art Report 7*, Transportation Research Board.

Dowling, N.E. and J.A. Begley. (1976). "Fatigue crack growth during gross plasticity and the j-integral." *ASTM, STP 590*, 82.

Fabb, T.R.J. (1974). "The influence of mix composition, binder properties and cooling rate on asphalt cracking at low-temperature." *Proc., AAPT*, Vol. 43, 285-331.

FHWA. (1982). "Transverse cracking of asphalt pavements." *Report No. FHWA-TS-82-205*, FHWA.

Finn, F., C.L. Saraf, R. Kulkarni, K. Nair, W. Smith, and A. Abdullah. (1986). "Development of pavement structural subsystems." *NCHRP 291*.

Fromm, H.J., and W.A. Phang. (1972). "A study of transverse cracking of bituminous pavements." *Proc., AAPT*, Vol. 41, 383-423.

Haas, R. (1973). "A method for designing asphalt pavements to minimize low-temperature shrinkage cracking." *RR-73-1*, Asphalt Institute.

Haas, R., F. Meyer, G. Assaf, and H. Lee. (1987). "A comprehensive study of cold climate airport pavement cracking." *Proc., AAPT*, Vol. 56, 198-245.

Haas, R., and T. Topper. (1969). "Thermal fracture phenomena in bituminous surfaces." *Special Report No. 101*, Highway Research Board, Washington, D.C.

Haas, R., and W. Phang. (1988). "Relationships between mix characteristics and low-temperature pavement cracking." *Proc., AAPT*, Vol. 57, 290-319.

Hadipour, K., and K.O. Anderson. (1988). "An evaluation of permanent deformation and low temperature characteristics of some recycled asphalt concrete mixtures." *Proc., AAPT*, Vol. 57, 615-645.

Heukelom, W. (1966). "Observation on the rheology and fracture of bitumens and asphalt mixes." *Proc., AAPT*, Vol. 35, 358-399.

Heukelom, W. (1969). "A bitumen test data chart for showing the effect of temperature on the mechanical behavior of asphaltic bitumens." *Journal of the Institute of Petroleum*.

Heukelom, W., and A. Klomp. (1964). "Road design and dynamic loading." *Proc., AAPT*, Vol. 33, 92-125.

- Hills, J.F., and D. Brien. (1966). "The fracture of bitumens and asphalt mixes by temperature induced stresses." *Proc., AAPT*, Vol. 35, 292-309.
- Humphreys, J., and C. Martin. (1963). "Determination of transient thermal stresses in a slab with temperature-dependent viscoelastic properties." *Transactions of the Society of Rheology*, Vol. 7.
- Hutchinson, J.W., and P.C. Paris. (1979). "Stability analysis of j-controlled crack growth." *ASTM, STP 668*, 37.
- Janoo, V. (1989). "Performance of 'soft' asphalt pavements in cold regions." USA CRREL Special Report.
- Jones, G.M., M.I. Darter, and G. Littlefield. (1968). "Thermal expansion-contraction of asphaltic concrete." *Proc., AAPT*, Vol 37, 56-100.
- Kallas, B.F. (1982). "Low-temperature mechanical properties of asphalt concrete." Asphalt Institute Research Report, No. RR-82-3.
- Kandhal, P.S. (1979). "Evaluation of six AC-20 asphalt cements by use of the indirect tensile test." *Transportation Research Record*, No. 712, 1-8.
- King, G.N., H.W. King, O. Harders, P. Chaverot. (1988). "Low temperature benefits of polymer modified asphalts." *Proc., Canadian Technical Asphalt Association*, Vol. 33, Calgary, Alberta.
- Landes, J.D. and J.A. Begley. (1976a). "Recent developments in  $J_{IC}$  testing." Westinghouse R&D Center, *Westinghouse Scientific Paper 76-1E7-JINTF-P3*, Pittsburgh, PA.
- Landes, J.D. and J.A. Begley. (1976b). "Mechanics of crack growth." *ASTM STP 590*, 128-148.
- Little, D.N. and K. Mahboub (1985). "Engineering properties of first generation plasticized sulfur binders and low temperature fracture evaluation of plasticized sulfur paving mixtures," *Transportation Research Record*, No. 1034, 103-111.
- Littlefield, G. (1967). "Thermal expansion and contraction characteristics - Utah asphaltic concretes." *Proc., AAPT*, Vol. 36, 673-697.
- Lytton, R.L., U. Shanmugham, and B. Garrett. (1983). "Design of flexible pavements for thermal fatigue cracking." *Research Report No. 284-4*, Texas Trans. Inst., Texas A&M University.
- Lytton, R.L., and U. Shanmugham. (1982). "Analysis and design of pavements to resist thermal cracking using fracture mechanics." *Proc., 4th Intl. Conf. on Structural Design of Asphalt Pavements*, Univ. of Michigan.
- Mahboub, K. (1985). "Low temperature fracture evaluation of plasticized sulfur paving mixtures," M.S. Thesis submitted to Texas A&M University.
- Majidzadeh, et al. (1977). "Development and field verification of a mechanistic structural design system in Ohio." *Proc., 4th Intl. Conf. on Structural Design of Asphalt Pavements*, Univ. of Michigan.

Majidzadeh, K., C. Buranrom and M. Karakomzian. (1976). "Applications of fracture mechanics for improved design of bituminous concrete." *Report No. 76-91*, FHWA, U.S. Dept. of Transportation.

Marek, C.R., Editor. (1976). "Low temperature properties of bituminous materials and compacted bituminous paving mixtures." *ASTM STP 628*.

McLeod, N.W. (1972). "A four year survey of low temperature transverse pavement cracking on three Ontario test roads." *Proc., AAPT*, Vol. 41, 424-493.

McLeod, N.W. (1987). "Pen-Vis Number (PVN) as a measure of paving asphalt temperature susceptibility and its application to pavement design." *Proc., Paving in Cold Areas Workshop*, Vol. 1, pp. 147-240.

Monismith, C.L., G.A. Secor, and K.E. Secor. (1965). "Temperature induced stresses and deformations in asphalt concrete." *Proc., AAPT*, Vol. 34, 248-285.

Osterkamp, T.E., G.C. Baker, B.T. Hamer, J.P. Gosink, J.K. Peterson, And V. Gruol. (1986). "Low temperature transverse cracks in asphalt pavements in interior Alaska." *Report AD-RD-86-26*, Alaska Department of Transportation.

Rice, J.R. (1968a). "A path independent integral and the approximate analysis of strain concentration by notches and cracks." *Journal of Applied Mechanics*, Vol. 35, 379.

Rice, J.R. (1968b). In: *Treatise on Fracture*, H. Liebowitz, Second Edition, Academic Press, New York, 191.

Rice, J.R., and G.F. Rosengren. (1968). "Plane strain deformation near a crack tip in a power-law hardening material." *Journal of Mechanics and Physics of Solids*, Vol. 16, 1-12.

Roque, R., and B.E. Ruth. (1987). "Materials characterization and response of flexible pavements at low temperatures." *Proc., AAPT*, Vol. 56, 130-167.

Ruth, B.E. (1977). "Prediction of low-temperature creep and thermal strain in asphalt concrete pavements." *ASTM STP 628*, 68-83.

Ruth, B.E., L.L. Bloy, and A.A. Avital. (1982). "Prediction of pavement cracking at low temperatures." *Proc., AAPT*, Vol. 51, 53-103.

Scherocman, J.H. (1987). "International state-of-the-art colloquium on low temperature asphalt pavement cracking." *Proc., USA CRREL*.

Schmidt, R.J. (1975). "Use of ASTM tests to predict low-temperature stiffness of asphalt mixes." *Transportation Research Record 544*, TRB, National Research Council, Washington, D.C., 35-45.

Schmidt, R.J., and L.E. Santucci. (1966). "A practical method for determining the glass transition temperature of asphalt and calculation of their low temperature viscosities." *Proc., AAPT*, Vol. 35, 61-90.

Shahin, M.Y., and B.F. McCullough. (1972). "Prediction of low-temperature and thermal-fatigue cracking in flexible pavements." *Report No. 123-14*, CFHR, University of Texas.

Shahin, M.Y., and B.F. McCullough. (1974). "Damage model for predicting temperature cracking in flexible pavements." *Record 521*, Transportation Research Board, 30-46.

Sugawara, T., and A. Moriyoshi. (1984). "Thermal fracture of bituminous mixtures." *Proc., Paving in Cold Areas Mini-Workshop*, 291-320.

Transportation Research Board. (1989). "Consistency, setting rate, and temperature susceptibility of asphalts; 1960-1987 annotated bibliography." *Biography 64*, National Research Council, Washington, DC.

Tuckett, G.M., G.M. Jones, and G. Littlefield. (1970). "The effects of mixture variables on thermally induced stresses in asphaltic concrete." *Proc., AAPT*, Vol. 39, 703-744.

van der Poel (1954). "A general system describing the viscoelastic properties of bitumens and its relation to routine test data." *Journal of Applied Chemistry*, Vol. 4.

Von Quintus, H.L., J.A. Scherocman, C.S. Hughes, and T.W. Kennedy. (1988). "Development of asphalt-aggregate mixture analysis system: AAMAS." Phase II - Vol. I, Preliminary Draft of Final Report.